REPUBLIC OF TURKEY
YILDIZ TECHNICAL UNIVERSITY
GRADUATE SCHOOL OF NATURAL AND APPLIED SCIENCES

FABRICATION OF CARBON NANOTUBE REINFORCED PLASTIC MATRIX COMPOSITES USING 3 DIMENSIONAL PRINTING

ALTUĞ AKPINAR

MSc. THESIS
DEPARTMENT OF MECHANICAL ENGINEERING
PROGRAM OF MANUFACTURING

ADVISER
ASST. PROF. DR. BEDRİ ONUR KÜÇÜKYILDIRIM

İSTANBUL, 2017

REPUBLIC OF TURKEY

YILDIZ TECHNICAL UNIVERSITY

GRADUATE SCHOOL OF NATURAL AND APPLIED SCIENCES

FABRICATION OF CARBON NANOTUBE REINFORCED PLASTIC MATRIX COMPOSITES USING 3D PRINTINGS

A thesis submitted by Altuğ AKPINAR in partial fulfillment of the requirements for the degree of **MASTER OF SCIENCE** is approved by the committee on 14.12.2017 in Department of Mechanical Engineering, Manufacturing Program.

Thesis Adviser

Asst. Prof.Dr. Bedri Onur KÜÇÜKYILDIRIM

Yıldız Technical University

Approved By the Examining Committee

Asst. Prof. Dr. Bedri Onur KÜÇÜKYILDIRIM

Yıldız Technical University _____

Asst. Prof. Dr. Binnur SAĞBAŞ

Yıldız Technical University _____

Assoc. Prof. Dr. Emel TABAN

Kocaeli University _____

ACKNOWLEDGEMENTS

This thesis, which is about the 3D printed nanocomposite material, is a result of dedicated work that realized in Yıldız Technical University (YTU), Istanbul, Turkey which is hardly possible without people who had supported me.

First of all, I would like to express my sincere thanks to my thesis advisor Dr. Bedri Onur KÜÇÜKYILDIRIM who guides and supports me in all meanings. His behaviors and supports always make me motivated and ardent even in compelling circumstances in this scientific work.

I would like to thank every member of YTU - Advanced Material Research Group; in addition I express many thanks to Metehan DEMİRKOL and Doğanbarış GÜNDOĞAN who spend their precious hours with me during the process of experiment. Moreover, I thank graduate students Gürkan BALKIS and Nergis YILMAZ who assisted me in the most hazardous part of my experiments as a part of their Machine Design.

The last but not the least, I would like to thank my mother Serpil, my father Devrim and my brother Anıl for their help. They always support me unconditionally in all situations. I couldn't progress so much without their existence and patience. Their unconditional support and love encourage me to go further in my life. I owe them so many things in my life that I can barely thank them in one paragraph. Furthermore, I would like to thank to my lovely supporter Melis who enlighten my life with her existence.

November 2017

Altuğ AKPINAR

TABLE OF CONTENTS

Page

LIST OF SYMBOLS iv

LIST OF ABBREVIATIONS v

LIST OF FIGURES iv

LIST OF TABLES vi

ABSTRACT vii

ÖZET ix

CHAPTER 1

INTRODUCTION 1

1.1 Literature Review 1
1.2 Purpose of Thesis 2
1.3 Contribution to Original Knowledge 3

CHAPTER 2

CARBON NANOTUBES 5

2.1 Element of Carbon 5
2.2 Allotropes of Carbon 6
2.3 Carbon Nanotubes 7
2.3.1 Introduction 7
2.3.2 Structure 8
2.3.3 Mechanical Properties 11

CHAPTER 3

3D PRINTING 14

3.1 Introduction 14
3.2 Working Principle 15
3.3 Types of 3D Printing Technologies 20
3.4 Stereolithography 21

CHAPTER 4

COMPOSITE MATERIALS 27

4.1 Introduction 27
4.2 Classification of Composite Materials 27
4.2.1 Polymer Matrix Composites 27
4.2.2 Metal Matrix Composites 28
4.2.3 Ceramic Matrix Composites 28
4.3 Vat Photopolymerisation 29
4.4 Fabrication of Carbon Nanotube Reinforced Polymer Composites 30

CHAPTER 5

EXPERIMENTAL STUDIES 32

5.1 Introduction 32
5.2 Materials and Tools 33
5.3 Functionalization of Carbon Nanotubes 37
5.4 Preparation of Nano Composite Resin and Sedimentation Test 44
5.5 Printing Nanocomposite 47
5.6 Mechanical Tests 48
5.6.1 Tensile Test 48
5.6.2 Wear Test 49
5.6.3 Results and Discussion 53

CHAPTER 6

CONCLUSION 61

REFERENCES 62

APPENDIX-A

GRAPHS OF EXPERIMENTAL STUDIES 67

CURRICULUM VITAE 89

LIST OF SYMBOLS

Å	Ångstrom
σ	Sigma (bond)
π	Pi (bond)
MPa	Mega Pascal
GPa	Giga Pascal
TPa	Tera Pascal
m	Meter
cm	Centimeter
mm	Millimeter
µm	Micrometer
nm	Nanometer
g	Gram
˚C	Celsius Degree
mL	Milliliter

LIST OF ABBREVIATIONS

2D	2 Dimensional
3D	3 Dimensional
3DP	3 Dimensional Printing
ABS	Acrylonitrile Butadiene Styrene
CAD	Computer Aided Design
CMC	Ceramic Matrix Composites
CNC	Computer Numerical Control
CNT	Carbon Nanotube
CVD	Chemical Vapor Deposition
DLD	Direct Laser Deposition
FDM	Fused Deposition Modeling
FEM	Finite Elemental Analysis
FT-IR	Fourier Transform Infrared Spectroscopy
IR	Infrared
LOM	Laminated Object Manufacturing
MD	Molecular Dynamics
MMC	Metal Matrix Composites
MIT	Massachusetts Institute of Technology
MWCNT	Multi Walled Carbon Nanotube
MWNT	Multi Walled Nanotube
PLA	Poly Lactic Acid
PMC	Polymer Matrix Composites
PVA	Polyvinyl Alcohol
RP	Rapid Prototype
SEM	Scanning Electron Microscope
SLA	Stereolithography
SLS	Selective Laser Sintering
SWCNT	Single Walled Carbon Nanotube
SWNT	Single Walled Nanotube
TEM	Transmission Electron Microscope
TPM	Tripropylene Glycol Monomethyl Ether
UV	Ultraviolet
VP	Vat Polymerization

LIST OF FIGURES

Page

Figure 2.1 Allotropes of carbon 7
Figure 2.2 The graphene sheet labeled with the integers (n, m). The diameter, chiral angle, and type can be determined by knowing the integers (n, m). 9
Figure 2.4 MD simulation of a large-amplitude transverse deformation of a carbon nanotube [22]. 12
Figure 3.1 Three types of fundamental fabrication processes 16
Figure 3.2 Process chain of RP 17
Figure 3.3 An illustration of the SLA process 22
Figure 3.4 Commercial SLA machines. (Formlabs Inc., Formlabs Form 2+) 23
Figure 3.5 SLA process step-by-step 24
Figure 3.6 An SLA model of a dashboard part. 25
Figure 3.7 The cone features generated by the laser curing process resulting in uncured regions throughout the part. 25
Figure 4.1 Schematic diagrams of three approaches to photopolymerisation processes 30
Figure 5.1 Scheme of experimental study 32
Figure 5.2 SEM image of MWCNT as received 34
Figure 5.3 TEM image of MWCNT as received 35
Figure 5.4 TGA/DTA analysis results of MWCNT as received 36
Figure 5.5 Chemically functionalization of CNT [52] 38
Figure 5.6 Sonication of CNT in ultrasonic bath 38
Figure 5.7 CNTs after sonication 39
Figure 5.8 Reflux system 40
Figure 5.9 Diluted CNT mixture 40
Figure 5.10 Filtration system 41
Figure 5.11 Perkin Elmer Spectrum 100 42
Figure 5.12 FT-IR result of pristine CNT. 43
Figure 5.13 FT-IR result of functionalized CNT 43
Figure 5.14 Sedimentation test images of CNT in resin. 46
Figure 5.15 Formlabs 2+ SLA type 3D Printer 47
Figure 5.16 Specimens with support structures. 48
Figure 5.17 Electro-mechanical Testing Device used for Tensile Tests 49
Figure 5.18 Tensile Test Specimens 49

Figure 5.19 Tribotechnic Pin-on-Disk Tribotester 50
Figure 5.20 Disc type wear test specimen of base material.....50
Figure 5.21 Disc type wear test specimen of CNT reinforced composite material 51
Figure 5.22 Macroscope 52
Figure 5.23 SEM Images of base tensile test specimen surface 54
Figure 5.24 SEM Images of reinforced tensile test specimen surface.....56
Figure 5.25 SEM Image of base test specimen.....59
Figure 5.26 SEM Image of base test specimen.....60

LIST OF TABLES

Page

Table 3.1 Parameters used in the SLA process 19
Table 3.2 Essential post processing tasks for different RP processes 20
Table 5.1 Chemical analysis of CNT 34
Table 5.2 Properties of resin in solid phase 36
Table 5.3 Properties of resin in liquid phase 36
Table 5.4 Identified functional groups in CNT 44
Table 5.5 Tensile Test Results 53
Table 5.6 Calculated Wear Rate and Specified Wear Rate of Base Specimen 57
Table 5.7 Calculated Wear Rate and Specified Wear Rate of Reinforced Specimen 57
Table 5.8 Friction coefficients of specimen 58

ABSTRACT

FABRICATION OF CARBON NANOTUBE REINFORCED PLASTIC MATRIX COMPOSITES USING 3D PRINTING

Altuğ AKPINAR

Department of Mechanical Engineering

MSc. Thesis

Adviser: Asst. Prof. Dr. Bedri Onur KÜÇÜKYILDIRIM

Recently, many breakthrough manufacturing methods begin to appear. One of the most common among these methods is 3 dimensional printing which is based on additive manufacturing method. 3 dimensional printing gives us advantage of manufacturing parts in single process. Despite its advantages 3 dimensional printed products have limited mechanical properties. Due to that disadvantage, 3 dimensional printing methods are rarely used for manufacturing final products.

Carbon nanotubes are carbon based nano materials which have impressive mechanical properties. In literature, there are studies about polymer matrix carbon nanotube reinforced nano composites. In those studies, it is proved that if carbon nanotubes are functionalized and dispersed adequately, polymer matrix will have greatly enhanced mechanical properties. As these superior properties of carbon nanotubes are considered, carbon nanotubes reinforced nano materials have great potential to eliminate limitation of mechanical properties of 3 dimensional printing.

The aim of this study is to produce carbon nanotube reinforced resin for stereolithography type 3 dimensional printers in order to improve mechanical properties of printed products to make them available for final products. In this regard, carbon nanotubes are functionalized properly by chemical methods in order to prevent agglomeration and create

strong interface between carbon nanotubes and polymer matrix. Carbon nanotubes are dispersed in resin homogenously by ultrasonication method. As we prepared nano composite resin, we applied sedimentation test in order to determine stability of nano composite resin. As a result of test, sedimentation was not observed in short and long term in any ratio. Subsequently we manufactured tensile and wear specimens in order to evaluate mechanical properties of nano composite specimens. As a result of mechanical tests, we observe that tensile and wear properties of 3 dimensional printed products are enhanced dramatically.

As a result, we managed to prepare nano composite resin and manufactured specimens from nano composite resin. Our reinforced specimens show superior properties than base specimens. This study shows us that limited mechanical properties of 3 dimensional printed products can surpassed by using reinforcement of carbon nanotube which is processed adequately. As one of the most important problem of 3 dimensional printed products have solved, 3 dimensional printings can find itself more field of applications.

Keywords: Nano composite, 3 dimensional printing, Carbon nanotube, Stereolithography, Mechanical properties.

YILDIZ TECHNICAL UNIVERSITY

GRADUATE SCHOOL OF NATURAL AND APPLIED SCIENCES

ÖZET

3 BOYUTLU YAZICI KULLANARAK KARBON NANOTÜP TAKVİYELİ NANO KOMPOZİT ÜRETİMİ

Altuğ AKPINAR

Makine Mühendisliği Anabilim Dalı

Yüksek Lisans Tezi

Tez Danışmanı: Yrd. Doç. Dr. Bedri Onur KÜÇÜKYILDIRIM

Günümüzde pek çok yeni üretim yöntemi ortaya çıkmaya başlamıştır. Bu yöntemler arasında en çok adı duyulan yöntem, katmanlı üretim yöntemine dayanan 3 boyutlu yazıcı yöntemidir. Bu yöntem sayesinde geleneksel yöntemlerle tek seferde üretilmesi imkansız olan geometriler tek prosesle üretilebilmektedir. Bu avantajına rağmen 3 boyutlu yazıcılarla üretilen ürünler sınırlı mekanik özelliklere sahip olmaktadır. Bu sebepten dolayı 3 boyutlu yazıcı yöntemi son ürünü üretmek için nadiren kullanılmaktadır.

Karbon nanotüpler üstün mekanik özelliklere sahip karbon içeren nano malzemelerdir. Literatürde karbon nanotüp takviyeli polimer matrisli nano kompozitlerle ilgili çalışmalar bulunmaktadır. Bu çalışmalar göstermiştir ki; eğer karbon nanotüpler uygun şekilde fonksiyoneleştirilir ve matris içinde homojen biçimde disperse edilirse mekanik özelliklerin önemli ölçüde arttığı görülmüştür. Karbon nanotüplerin bu üstün mekanik özelliklerinden dolayı, 3 boyutlu yazıcılarda takviye malzemesi olarak kullanılabileceği bu sayede basılan parçaların mekanik özelliklerinin geliştirilebileceği öngörülmüştür.

Bu çalışmada stereyolitografi tipi 3 boyutlu yazıcılar için karbon nanotüp takviyeli reçine üretilerek, mekanik özelliklerin geliştirilmesi amaçlanmış olup; bu sayede 3 boyutlu yazıcılardan son ürünün elde edilebilmesi hedeflenmiştir. Bu çalışmada ilk olarak karbon nanotüpler aglomerasyonu önlemek ve matris malzemesi ile iyi bir ara yüzey oluşturmak

amacıyla kimyasal yöntemler ile fonksiyonelleştirilmiştir. Ardından karbon nanotüpler reçine içinde ultrasonik yöntemle homojen bir şekilde disperse edilmiştir. Hazırlanan nano kompozit çökelme testine tabi tutulmuştur. Çökelme testinin sonucunda herhangi bir çökelme görülmemiştir. Bu işlemlerin ardından mekanik özelliklerin belirlenmesi amacıyla çekme ve aşınma testi numuneleri hazırlanmıştır. Yapılan testler sonucunda 3 boyutlu yazıcıda basılan nano kompozit malzemenin çekme ve sürtünme özelliklerinde oldukça ileri seviyelerde artış gözlenmiştir.

Bu çalışmanın sonucunda; nano kompozit reçine hazırlanarak, deney numuneleri başarılı bir şekilde basılmıştır. Basılmış olan nano kompozit numuneler, katkısız numunelere kıyasla çok daha ileri özellikler göstermiştir. Bu çalışma bize göstermiştir ki 3 boyutlu yazılarda basılan parçaların sınırlı mekanik özellikleri uygun bir şekilde fonksiyonelleştirilmiş karbon nanotüp takviyesiyle elde edilmiş nano kompozit reçine kullanılarak geliştirilebilmektedir. Bu sayede 3 boyutlu yazıcılarda büyük bir problem olarak görülen sınırlı mekanik özellikler geliştirilmiştir. Bu gelişmelerin ışığında 3 boyutlu yazıcılar kendilerine daha geniş bir uygulama alanı bulabilecektir.

Anahtar Kelimeler: Nano kompozit, 3 boyutlu yazıcı, Karbon nanotüp, Steryolitografi, Mekanik özellikler.

CHAPTER 1

INTRODUCTION

1.1 Literature Review

Since CNT have discovered in 1991 [1], it became quite popular in science and engineering due to its physical and chemical properties. CNT have extraordinary mechanical properties and electrical properties. Before CNT, none other materials have combination of these superior properties. Due to their properties CNT have found large field of applications [2].

Extraordinary properties of CNT make it perfect candidate for reinforcement material for composites. Also its physiochemical properties make it excellent reinforcing material for polymers. Solid progresses have been done by adding carbon nanotube into polymer matrix to enhance its mechanical [3] and electrical properties [4]. The experiments show that CNT reinforced polymer have better properties in elastic modulus, tensile strength over pristine matrix modulus. Qian et al. [5] have shown that 1 wt% of CNTs increase elastic modulus between 36% to 42% and increase tensile strength about 25% in epoxy. Schadeler et al. [6] found that 5 wt% of CNTs increase elastic modulus by 40% percent in epoxy. Zhu et al. [7] observed the stress-strain curve of epoxy resin with CNT reinforcement ratio between 1 wt% and 4 wt% and they have found elastic modulus epoxy increase of 30% to 70%. Despite of its excellent properties there are some setbacks to use carbon nanotube into polymer matrix. The most important problem is untreated CNT has lack of functional group. That absence causes CNT particles are tend to aggregate with each other because of van der Waals force [8]. In order to improve dispersibility of CNT processed with covalent and non-covalent functionalization. As CNT ratio increases, it is expected that mechanical properties will be improved due to loading on CNT is increased. However two phase

structure and void defect between polymer and CNT, mechanical properties of composite will decline as ratio of CNT increases to a high proportion (>10 wt%)

3D printing may became popular in recent times but it was first described by Charles Hull in 1986. [9] 3D printed polymer products have limited mechanical properties due to their additive manufacturing method. In order to improve those mechanical properties polymer have reinforced by various materials. Zhong et al. [10] have reinforced Acrylonitrile Butadiene Styrene (ABS) for Fused Deposition Modeling (FDM) type printer with glass fiber (18 wt%) and tensile strength improved by 140%. Tekinalp et al. [11] have shown that ABS has reinforced by carbon fiber (40 wt%) and tensile strength improved by 115%. Compton et al have reinforced epoxy resin for direct writing method with carbon fiber and silicon carbide whisker (35 wt%) and improved tensile strength up to 127%. In other studies effects of continuous fibers on composites have shown. Van der Klift et al. [12] reinforced Nylon with continuous carbon fibers (34.5 vol%) and improved tensile strength by 446%. Matsuzaki et al. [13] have reinforced PLA with continuous fiber (6.6 vol%) and increased tensile strength by 335%) In FDM type printing systems 4% graphene oxide added in ABS matrix, as a result elastic modulus increased 30% and tensile strength increased by 32 % [14]. Lin et al. [15] have used SLA technology in order to have nanocomposite. They reinforced epoxy photopolymer resin with 0,2% graphene oxide, they improved tensile strength by 62,2 % and improved elongation by 12,8%. In study with CNT by FDM type 3D printer ABS matrix is reinforced by MWCNT by 3%, tensile modulus is increased by 63% [16]. In another study photopolymer epoxy resin used in SLA type 3D printer reinforced with 0,10% MWCNT and tensile strength increased by 7,5% and fracture stress increased by 33% [17].

1.2 Purpose of Thesis

Recently, many breakthrough manufacturing methods and processes appear. One of the most common and known among these methods is 3 Dimensional (3D) printing. 3D printing is a new kind of manufacturing method that based on additive manufacturing. It is one of the most popular and promising method in recent days. 3D printing owes its popularity to two main reasons. Firstly, 3D printing allows us to manufacture parts in single

process that they cannot be manufactured by traditional methods such as machining, casting or forming. The latter, 3D printing can even be used in places like homes and offices. By that way, every houses and offices may turn into small factories. Despite all these good sides, 3D printing has some serious drawbacks. Due to being an additive manufacturing method, goods manufactured by 3D printing has limited mechanical properties compared to some traditional methods as mold injection. Besides, 3D printing has a limited material variety for application and the most popular type of materials are used by 3D printers are polymers. Some 3D printing methods can process metals as well.

Composite materials are one of the best options to manufacture products by 3D printers with better mechanical properties. Because, reinforcing a matrix material is not only applicable but also very effective way to improve materials' mechanical properties if applied properly.

In composite materials, properties of material can be improved proportional to reinforcement ratio, reinforcement properties and matrix - reinforcement interface properties. In composite materials, if at least one of these phases is in nano scale it is called as nano composites. Nano composites have superior properties than the traditional composite materials. Especially, nano composites may have better properties even in lower reinforcement ratios.

Due to all these reason, we have objective to obtain homogeneous nano composite resin in order to manufacture products which have improved mechanical properties compared to resin. Therefore we aim to use MWCNT reinforced nano composite to improve tensile and wear properties material.

1.3 Contribution to Original Knowledge

This thesis is mainly examination of the aspect of fabrication of CNT reinforced nano composites by SLA type 3D printing. Resin preparation process has been studied for different CNT reinforcement ratios in order to achieve homogeneously distributed composite resins with minimum sedimentation. In following, fabricated specimens'

mechanical properties have been investigated and effects of CNT reinforcements are discussed.

Some of the most vital contributions to original knowledge achieved in this thesis are listed below;

(i) CNTs are dispersed by ultrasonication in thermosetting resin homogenously after the proper chemical functionalization process. In literature we do not run across this type of CNT surface modification process for 3D printing.

(ii) 3D printed nano composites show great mechanical improvements in means of tensile strength and wear resistance even with very low (0,02 wt%) CNT reinforcement ratio.

(iii) Fracture surfaces of specimens are examined by SEM and CNTs' effect on fracture mechanism are discussed. Moreover, wear mechanism on wear surfaces are identified by SEM examinations on 3D printed materials as well.

3D printed materials are mostly used in prototyping due to their poor mechanical properties. Result of this study shows us that mechanical properties will not be a restriction in industrial 3D printing applications by the usage of nano composite resins to be developed. It is clear that with proper functionalization process; even very low CNT reinforcement can increase the mechanical properties dramatically. Moreover, SLA type 3D printing has the best dimensional tolerances for printed products. By precision of SLA type 3D printing and increment of resins' mechanical properties, 3D printing methods can be used for manufacturing of final products

CHAPTER 2

CARBON NANOTUBES

2.1 Element of Carbon

Carbon is the most versatile element in the periodic table, owing to the type, strength, and number of bonds it can form with many different elements. The diversity of bonds and their corresponding geometries enable the existence of structural isomers, geometric isomers, and enantiomers. These are found in large, complex, and diverse structures and allow for an endless variety of organic molecules.

The properties of carbon are a direct consequence of the arrangement of electrons around the nucleus of the atom. There are six electrons in a carbon atom, shared evenly between the 1s, 2s, and 2p orbitals. Since the 2p atomic orbitals can hold up to six electrons, carbon can make up to four bonds. However, the valence electrons, involved in chemical bonding, occupy both the 2s and 2p orbitals.

Covalent bonds are formed by promotion of the 2s electrons to one or more 2p orbitals; the resulting hybridized orbitals are the sum of the original orbitals. Depending on how many p orbitals are involved, this can happen in three different ways. In the first type of hybridization, the 2s orbital pairs with one of the 2p orbitals, forming two hybridized sp1 orbitals in a linear geometry, separated by an angle of 180˚. The second type of hybridization involves the 2s orbital hybridizing with two 2p orbitals; as a result, three sp2 orbitals are formed. These are on the same plane separated by an angle of 120˚. In the third hybridization, one 2s orbital hybridizes with the three 2p orbitals, yielding four sp3 orbitals separated by an angle of 109.5˚. Hybridization of sp3 yields the characteristic tetrahedral

arrangements of the bonds. In all three cases, the energy required to hybridize the atomic orbitals is given by the free energy of forming chemical bonds with other atoms. Carbon can bind in a sigma (σ) bond and a pi (π) bond while forming a molecule; the final molecular structure depends on the level of hybridization of the carbon orbitals. An sp1 hybridized carbon atom can make two σ bonds and two π bonds, sp2 hybridized carbon forms three σ bonds and one π bond, and an sp3 hybridized carbon atom forms four σ bonds. The number and nature of the bonds determine the geometry and properties of carbon allotropes.

2.2 Allotropes of Carbon

Carbon in the solid phase can exist in three allotropic forms: graphite, diamond, and buckminsterfullerene. Diamond has a crystalline structure where each sp3 hybridized carbon atom is bonded to four others in a tetrahedral arrangement. The crystalline network gives diamond its hardness (it is the hardest substance known) and excellent heat conduction properties (about five times better than copper). The sp3 hybridized bonds account for its electrically insulating property and optical transparency. Graphite is made by layered planar sheets of sp2 hybridized carbon atoms bonded together in a hexagonal network. The different geometry of the chemical bonds makes graphite soft, slippery, opaque, and electrically conductive. In contrast to diamond, each carbon atom in a graphite sheet is bonded to only three other atoms; electrons can move freely from an unhybridized p orbital to another, forming an endless delocalized π bond network that gives rise to the electrical conductivity.

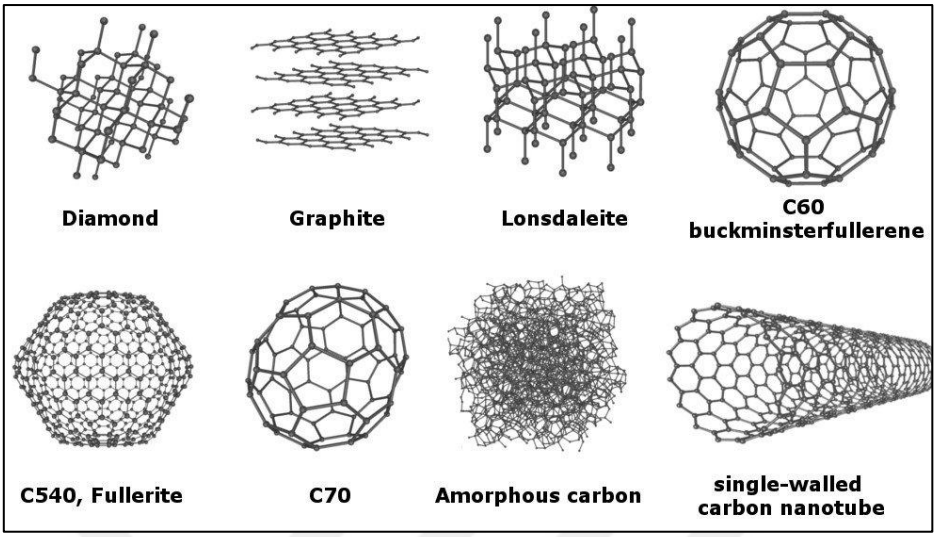

Figure 2.1 Allotropes of carbon

2.3 Carbon Nanotubes

2.3.1 Introduction

Carbon nanotubes were discovered in 1991 as a minor byproduct of fullerene synthesis [1]. Remarkable progress has been made in the ensuing 14 years, including the discovery of two basic types of nanotubes (single-wall and multiwall); great strides have been taken in their synthesis and purification, identification of the fundamental physical properties, and the most important steps among are being taken toward realistic practical applications.

Carbon nanotubes are long cylinders of three coordinated carbon with 4 bonds, slightly pyramidalized by a curve [18] from the pure sp2 hybridization of graphene, toward the diamond-like sp3. A perfect tube is capped and closed at both ends by hemi-fullerenes and has no dangling bonds. A SWNT is one cylinder by itself, while MWNT consist of many nested cylinders whose successive radii differ by roughly the interlayer spacing of graphite. The minimum diameter of a stable freestanding SWNT is limited by curvature-induced strain to ~0.4 nm [19]. MWNT may have outer shells 30 nm in diameter, with varying numbers of shells, affording a range of empty core diameters. Their lengths are up to 3 mm have been reported [20]. Nanotubes are distinguished from less-perfect quasi-one-dimensional carbon materials by their well-developed parallel wall structure. Other

elements too can be made into nanotubes, so one often encounters the term “Single Walled Carbon Nanotube (SWCNT)” to distinguish them from non-carbon tubes. The unique feature of carbon nanotubes is that they exist in both metallic and semiconducting properties.

SWNTs can be described as seamless cylinders rolled up from graphene rectangles from edges. C_{70} is the smallest nanotube; compared with C_{60} it contains an extra belt of hexagons normal to the fivefold axis of the hemi-C_{60} caps. Adding more belts leads to longer tubes of the metallic (5,5) armchair category as defined later. According to theory, cylindrical fullerene isomers are less stable than the more nearly spherical ones because the 12 pentagons necessary to ensure closure are localized on the two caps. These results in strain concentrations at the ends of closed tubes, which in turn makes it easier to perform additional chemistry on the ends than on the sidewalls.

2.3.2 Structure

Iijima was first to recognize Carbon Nanotubes (CNT) were rolled graphene sheet with numerous of helicities and chiralities rather than a graphene sheet rolled up as scroll. Iijima observed only MWNT with between 2 to 20 layers. However in subsequent publication in 1993, he confirmed existence of SWCNTs and elucidated their structure [21].

A SWCNT is rolled graphene tube. Observations of SWCNT show that growth mechanism is not like proper roll, the way graphene rolled determines the fundamental properties of the tube. In order describe the characteristic of CNT, two vectors refer as C_h and T, whose rectangle defines the unit cell, can be defined. C_h is a vector that defines circumference of the tube connecting two carbon atoms,

$$C_h = n\hat{a}_1 + n\hat{a}_2 \tag{2.1}$$

where â1 and â2 are the two basis vectors of graphite and n and m are integers.

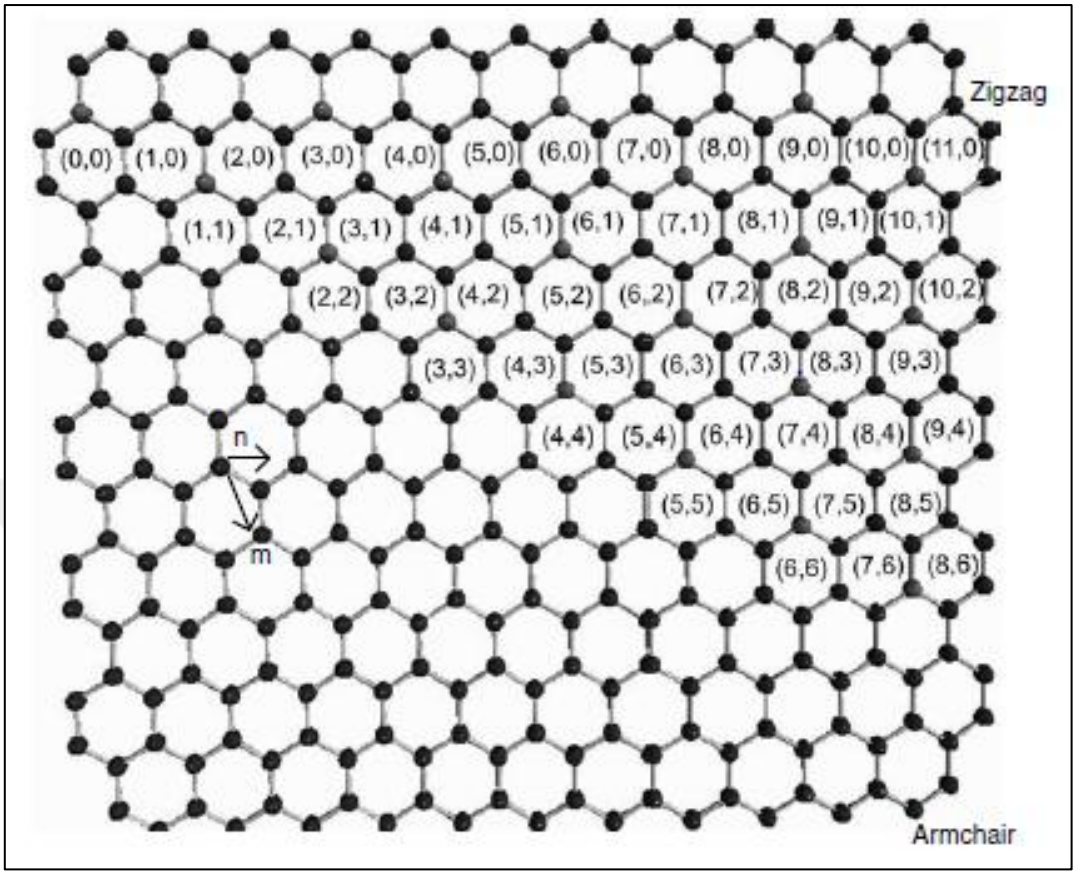

Figure 2.2 The graphene sheet labeled with the integers (n, m). The diameter, chiral angle, and type can be determined by knowing the integers (n, m).

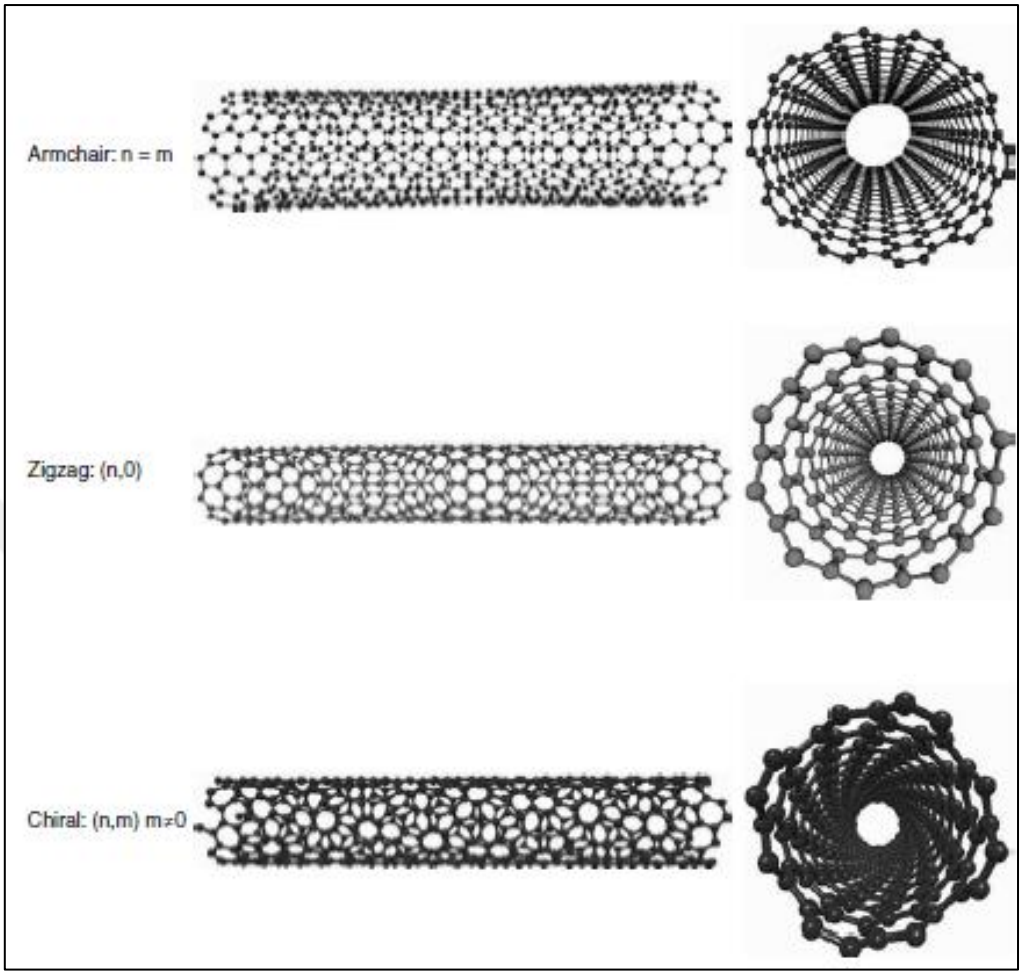

Figure 2.3 The graphene sheet labeled with the integers (n, m). The diameter, chiral angle, and type can be determined by knowing the integers (n, m).

n and m are called as indexes and determine the chiral angle;

$$\theta = tan^{-1} = (\sqrt{3}\left(\frac{n}{2m+n}\right)) \tag{2.2}$$

The chiral angle is used to separate carbon nanotubes into three different classes differentiated by their vital electronic properties: armchair ($n = m, \theta = 30^\circ$), zig-zag ($m = 0$, $n > 0$, $\theta = 0^\circ$), and chiral ($0 < |m| < n$, $0 < \theta < 30^\circ$). Armchair carbon nanotubes have metallic properties. (a degenerate semimetal with zero band gap). Zig-zag and chiral nanotubes can have semimetal properties with a finite band gap if $n - m/3 = i$ (i being an integer and $m \neq n$) or can be semiconductors in all other cases. The band gap for the semimetallic and semiconductor nanotubes scales approximately with the inverse of the

tube diameter, giving each nanotube a unique electronic behavior. The diameter of the nanotube can be expressed as;

$$d_t = \sqrt{3}[a_{c-c}(m^2 + mn + n^2)^{1/2}/\pi] = C_h/\pi \quad (2.3)$$

where C_h is the length of C_h, and a c-c is the C-C bond length which refers length bond between carbon atoms. (1,42 Å). Combining different diameters and chiralities results in several hundred individual nanotubes, each with its own distinct mechanical, electrical, piezoelectric, and optical properties

2.3.3 Mechanical Properties

The strength of carbon-carbon bonds gives extreme interest in mechanical properties of CNT. It should be stiffer and stronger than in any material theoretically. Simulations [22] and experiments [23] show a remarkable "bend, don't break" response of individual SWNT to large transverse deformations; an example from Yakobson's simulation is shown in Figure 2.4. The two segments on either side of the buckled region can be bent into an acute angle without breaking bonds; simulations and experiments show that once force is removed from SWCNT full recovery is provided and ensured.

Elastic modulus of a cantilevered individual MWCNT was measured between 1.0 to 1.8 TPa from the amplitude of thermally driven vibrations observed in the Transmission electron microscope (TEM) [24]. This is only 20% better than the best high-modulus graphite fibers. Exceptional resistance to shock loads has also been demonstrated [25]. Both modulus and strength are highly dependent on the nanotube growth method and subsequent processing because each of these processes has different variable and defects. Values of elastic modulus as low as 3 to 4 GPa have been observed in MWCNT produced by pyrolysis of organic precursors [26]. TEM-based pulling and bending tests gave more reasonable modulus and strength of MWNT as 0.8 and 150 GPa, respectively [27].

MWCNT and SWCNT bundles may be stiffer in bending but they are expected have lower properties under tension due to pullout of tubes. In one experiment, SWCNT bundles was broken under stress under 5,3 % strain. It can be understood from stress-strain curves that

load is carried by periphery of SWCNT ropes and breaking stress are read between 13 to 52 GPa. [28]. This is far less than that reported for a single MWNT [27]. On the other hand mean value of tensile modulus is 1 TPa with near-ideal behavior.

On the other hand, the mean value of tensile modulus was 1 TPa, consistent with near-ideal behavior. Clearly the effects of non-ideal structure have widely different influences on modulus and strength because there is ambiguity to choosing the proper cross sectional area to stress strain data. On a density-normalized basis the CNT look better [29]; modulus and strength are, respectively, 19 and 56 times better than steel.

Figure 2.4 shows the formation of a remarkable CNT by pulling and (optionally) twisting material from a "forest" of vertically aligned MWCNT grown by a CVD process [30]. The untwisted yarns are quite weak; if they accidentally touch a surface while being pulled off the substrate, they break immediately. On the other hand, twisted single-strand yarns show strengths between 150 to 300 MPa; this improved to 250 to 460 MPa in the two-ply yarns.

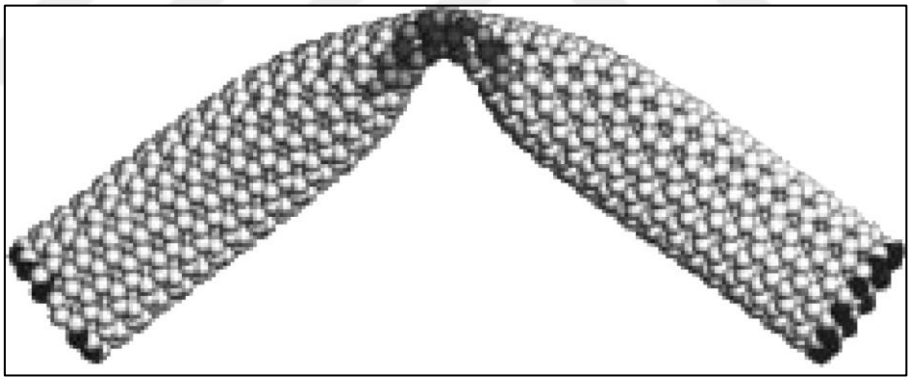

Figure 2.4 MD simulation of a large-amplitude transverse deformation of a carbon nanotube [22].

In some others experiments, 850 MPa was achieved by infiltration with PVA [30], which also improved the strain-to-failure to 13%. Toughness, the so-called "artificial muscle" [31], is a major issue in CNT based actuators. Another form of nanotube material that can be useful for sensors and actuators are thin film or buckypapers.

Another form of nanotube material useful for sensors and actuators are thin films or buckypapers. An ordinary results for solution-cast film with random SWCNT orientations in the plane [32] is described in [33]. Tensile modulus, strength and elongation to break

values are 8 GPa in 0,2 % strain and 30 MPa in 0,5 % respectively. This result is lower than what can achieved by fibers. It suggests us that failure in the films occurs via interfibrillar slippage rather than fracture within a fibril

CHAPTER 3

3D PRINTING

3.1 Introduction

3D printing technology has improved quite fast since it was presented and developed especially after 2000's. The first study about 3D printing technology was made and patented by Dr. Hideo Kodama in Japan and this technology presented as RP (rapid prototyping) technology [34]. Dr. Hideo Kodama was the first person who studied and presented 3D printing technology. However first working 3D printer was invented by Charles Hull based on Stereolithography (SLA) method in 1984.[9]. He developed a 3D printer by modifying tradition 2D inkjet printer. Following these events Hull co-founded 3D System Cooperation which is one the most procreative and innovative organizing operating in 3D printing sector today. Today many of these 3D printing concepts and technologies are patented by Hull. Until 1987 this 3D printed technique was the only technology in 3D printing. An new technology called as Selective Laser Sintering (SLS) was developed and patented by Carl Deckard in US [35]. However SLS will not be last technology will be presented; in 1989 FDM technology appeared. It was patented by Scott Crump and issued in 1992. Also this technology represented many of the entry level machines in 3D printing based on RepRap ((Replication Rapid-Prototyper Project) model. FDM in 3D printing is the most popular model in the world today. At end of the 80's and beginning of 90's 3D printing was only used RP. It has been the main of 3D printing since it was developed in order to create prototypes faster with less cost. This technology offers to examine objects' applicability and compatibility. With benefit of this breakthrough

technology product development became easier with fewer errors and cheaper. Consequently waste of money due to designation error minimized.

At the beginning of the 90's, 3D system Corporation and Massachusetts Institute of Technology (MIT) were leaders in 3D Printing Technology. Developers from MIT Michael Cima and Emmanuel Sachs invented "3 dimensional printing techniques" called 3DP. It is similar technology in inkjet 2D printer technology. This technology patented in 1993. In following MIT licensed its patents to 6 corporations and they started to develop based on 3DP technology. Earlier 3D printer was unaffordable and not convenient for general and mid-range market. However as this technology gradually become popular and developed market cost was decreased. This advance makes 3D printer more accessible and affordable. As a result printing technology was developed even faster in means printing speed, cost and printing resolution. Moreover range of material was increased from polymer to metal. By these improvements 3D printing were getting as small as we can use on desktop. Today 3D printing is being used in industry and household applications. Field of application is growing exponentially and involves extensive scale of disciplines. Today 3D printers are pushing limits of technology, design and innovation.

3.2 Working Principle

There are three fundamental fabrication processes [36] as shown in Figure 3.1. These processes are subtractive, additive and formative processes. Subtractive process is based on removal of unwanted material on base material until desired shape of object is reached. In contrast, an additive process is exactly reverse of subtractive process, larger materials are added each other until desired shape is reached. Lastly formative process is one where mechanical forces are applied with restrictive shape so as to form a desired shape. These processes are fundamental of manufacturing processes. Subtractive process include most of the machining process such as CNC milling, turning, cutting, drilling, water jet cutting, laser cutting, sawing etc. Most form of RP processes are also subtractive processes such SLA, SLS and FDM. Example of forming processes is bending, forging, plastic injection molding and drawing.

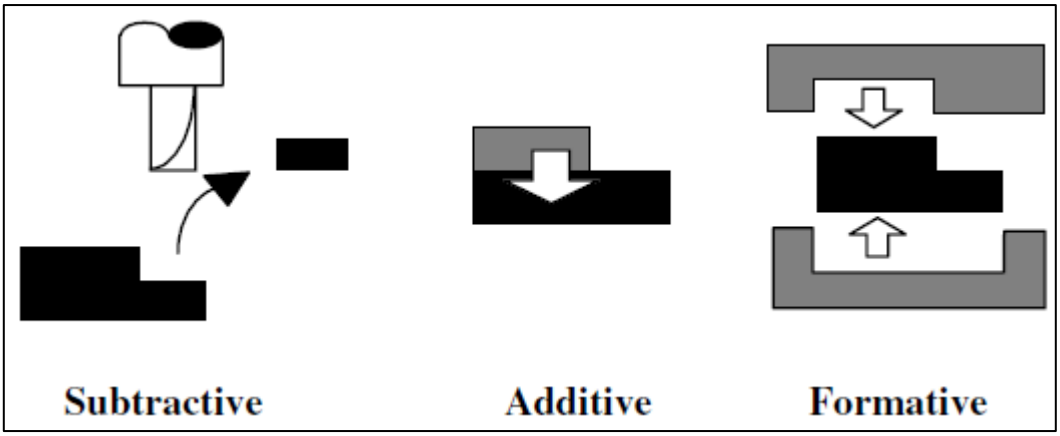

Figure 3.1 Three types of fundamental fabrication processes

All RP technologies have similar basic approach. As such all RP system generally have similar process chain. This generalized process chain is shown in Figure 3.2.. There are total seven steps in this chain. These steps are 3D modeling, data conversation, and transmission, preparing support structures, building and post processing.

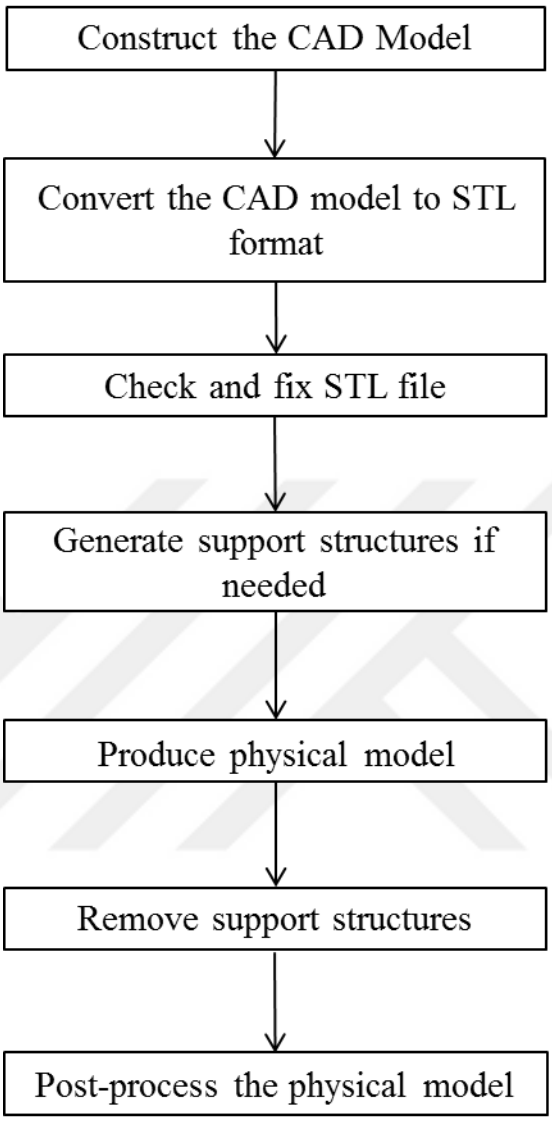

Figure 3.2 Process chain of RP

Like other fabrication processes, process planning is important before the RP commences. In process planning RP process chain are listed. The first step is creating a 3D modeling that requires workstation and 3D modeling software. The various factors and parameters which influence of performance of process are examined in this section.

Advanced 3D CAD modeling is the first part of RP processes and generally the most time consuming part of whole process in chain. It is most important that 3D models can be shared by entire design team to have FEM analysis, detail design, drafting and planning for

manufacturing. Many CAD/CAM systems have a 3D geometric modeler in order to use in special purpose such as creating supports.

After solid or surface model built, next step is to convert it into STL files.. This format gets his name from stereolithography which pioneers 3D printing. In STL files format approximates the surface using tiny triangles. Although linear surface can be identified by few triangles, curved surface need many more triangle. As a result curvy parts are likely to be very large. Today most of the 3D Modeling systems have STL conversion interface. Therefore conversation of 3D data into STL files is the easiest part of process chain. However highly complex structures may need even hours in low performance workstations. In some application support structures can be saved as separate files where supports are created by third party software by manufacturer. Transmission is step is also fairly easy, it only need to transfer data from computer to RP machine's computer where they may be in different locations.

Once STL files are checked in means of error, the RP system's computer analyzes STL files that define model to be fabricated and slice the model into cross-sections. The cross sections are created model slice by slice. Cross sections are fabricated onto previous one to form 3D model. Thickness of cross section can vary. In SLA thickness of each cross section can between 0,12 mm to 0,50 mm. In order to fabricate accurate model thickness have to be in lower value as cost of time. Support structure can be fabricated in coarser layer thickness because at the end of the process they will cut away.

Preparing building parameters for positioning and stepwise manufacturing in light of so many available parameters can be a challenge if not guided by proper documentation. These parameters might be determination of geometrical object, spatial assortment, and arrangement with other parts and slice parameters. In SLA may also have more parameters such as cure depth and laser power. As many vendors continually develop new systems, such parameters are less challenging for users. By these software products those parameters optimized automatically. Before this product is introduced, user has to set all these parameters by themselves. This was very tedious and time consuming work. These parameters are shown in Table 3.1.

Table 3.1 Parameters used in the SLA process

1. X-Y Shrink
2. Z Shrink
3. Number of copies
4. Multi part spacing
5. Range manager (add delete, etc.)
6. Recoating
7. Slice output scale
8. Resolution
9. Layer thickness
10. X–Y hatch-spacing or 60/120 hatch spacing
11. Skin fill spacing (X, Y)
12. Minimum hatch intersecting angle

The final task of RP systems are post processing task. At this point of task operation may vary related to fabrication methods. This stage need some manual hand work, as a result the danger of damaging part is high. Therefore, the operator has high responsibility to realization of part. On the other hand not all RP systems need all kind of post processing. The necessity of post processing is shown in Table 3.2.

The cleaning task refers for the removal of support structures or any other excess parts. Ln SLA it might be cleaning of excess liquid that trapped in blind holes. Similar in SLS it might clean of excess dust that remains on part. Likewise for LOM, pieces of excess wood or block of paper have to be removed which acts as support structures.

Table 3.2 Essential post processing tasks for different RP processes

Rapid Prototyping Technologies				
Postprocessing Tasks	SLS	SLA	FDM	LOM
1. Cleaning	✓	✓	X	✓
2. Postcuring	X	✓	X	X
3. Finishing	✓	✓	✓	✓

As shown in Table 3.2, the SLA process needs highest number of post processing task. More importantly for safety reason, specific recommendations for post process task have to be preparing SLA fabricated part. It was reported in research that accuracy is related with post treatment process [37]. After fabricated part is completed unreacted resin have to be cleaned. This excess resin is cleaned various solvents but solvent that used for cleaning may still damage or deform model. In order to give no damage to model newer cleaning solvents appear, like TPM (tripropylene glycol monomethyl ether) introduced by 3D Systems. With this solvent cleaning can be done with damage can be minimized or even eliminated.

Finishing task refers to secondary processes such as grinding and sanding in order to improve surface quality or even painting for either cosmetic reason or surface quality. It also includes machining process such as drilling and tapping in order add necessary feature to part.

3.3 Types of 3D Printing Technologies

3D printers are mainly divided into three class based on phases of their material, these are liquid, solid and powder [38].

Solid-based 3D printers are meant to encompass all forms of solid materials. Solid form can be used in wires, laminates and pellets. These techniques are mainly extrusion based FDM method, contour cutting and ultrasonic consolidations [39].

Liquid-based 3D printing has its initial materials in liquid state. Liquid based 3D printers have distinct advantage of smoothness of liquid surface in steady state, as a result in parts that fabricated by this method have better quality of surface. However material is limitation in these printing methods, because materials have to be solidified Most of the liquid based processes use heat sources to scan 2D surface of liquid. This process called as curing, the liquid is converted into a solid-state. The heat source, such as a UV laser, is chosen to control tiny spot to fabricate accurate materials. In general there are other ways to solidify liquid, a cold source the liquid point by point is an options. However not curing methods are possible for 3D printer. On the other hand these new approaches are opportunity to invent new 3D printing processes.

Powder based 3D printing are mostly used in metal materials. Direct laser deposition (DLD) and laser sintering processes belong to this category. These techniques are quite similar to other techniques but use different kind of material. They use laser for manufacturing. Generally the principle used is fusing a powder material and deposit it on wherever it needs to be.

3.4 Stereolithography

The SLA process is the commercial 3D printing process and is the representation of the SLA process. This process is patented in 1986. Henceforth SLA started the 3D printing revolution. Principle of this process is solidifying photosensitive resin by curing UV laser and fabricating 3D object layer by layer. SLA uses a photosensitive resin that mostly classified as epoxy, vinyl ether or acrylate. Materials have different curing behavior. For example Acrylics only cure about 70-80 % percent but epoxies continue to even after the laser is not contacting. Figure 3.3 shows that platform moves down as each layer is completed. The laser light moves in X and Y axis by a position control systems. In some cases support structures are need to be built overhanging part. In this experiment Formlabs

2+ SLA type 3D printer (Figure 3.4) is used in Open-Mode which is intended to use for vat polymerization instead of using cartridge.

SLA process converts 3D computer image date into very thin cross section of part. By that way parts will be sliced into hundreds or thousands of layers A platform that contains resin moves vertically. A laser beam traces a single layer onto surface of a vat of liquid photopolymer resin shown in Figure 3.5. The UV light causes to harden resin precisely where it contacts. As a shown in Figure 3.5a, the model is built upon a platform just below the surface in a vat filled with resin.

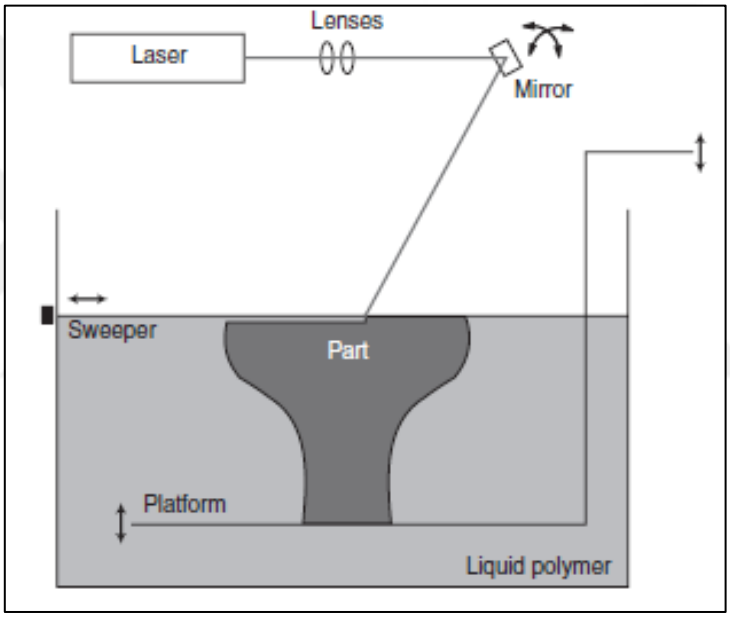

Figure 3.3 An illustration of the SLA process [38]

A low power but highly focused UV laser traces out first layer ,as shown in Figure 3.5b, solidifying liquid but leaving excess areas liquid. The UV laser is controlled by galvanometer scanner to generate X-Y motions and so platform does not need move in X-Y axis.

In the next step an elevator lower the platform incrementally into the resin as shown in Figure 3.5c. The laser is tracing from left. A sweeper recoats solidified part with resin and laser traces the second layer. This process is repeated until part is completed. (Figure 3.5d and 3.5e) Afterward solid removed from the vat and rinsed clean of excess liquid on part as

shown in Figure 3.5f. In all cases when part is built, there are small structures built on called as supports. Their purpose is to build overhanging part and creating bridge like structures. These supports touch part in very small point in order to be removed easily when the part is built. After support are broken by hand or cut. In some condition curing might be needed to improve mechanical properties further. The current SLA process has developed their technologies quickly. The Viper Pro SLA system by 3D systems has developed a SLA type 3D printer which has adjustable beam size to even faster fabrication.

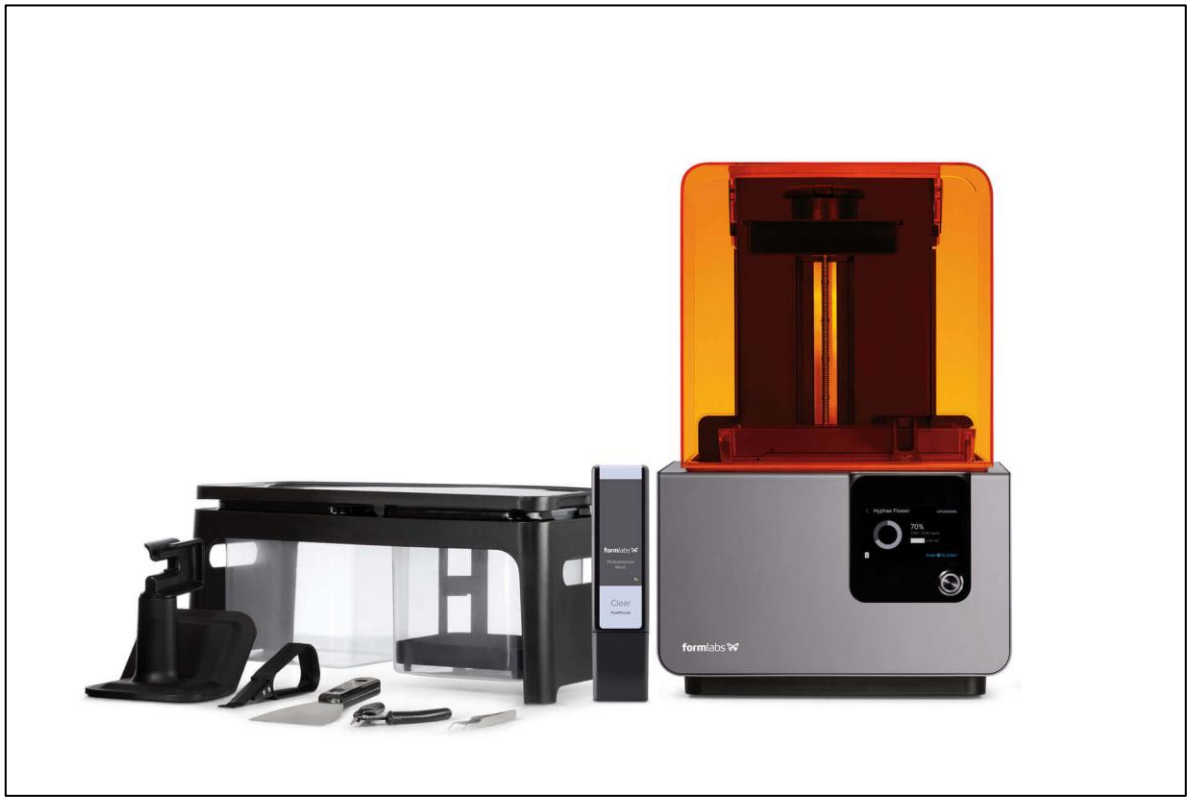

Figure 3.4 Commercial SLA machines. (Formlabs Inc., Formlabs Form 2+) [39]

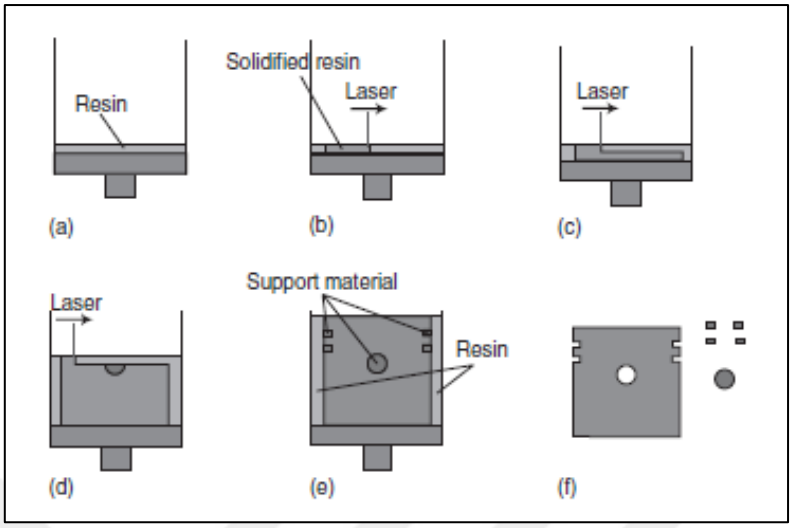

Figure 3.5 SLA process step-by-step: (a) a layer of resin to be solidified on a platform; (b) UV laser selectively traced out the first layer; (c) second layer with laser tracing from the left; (d, e) repeat to build the rest of the layers; (f) the final part after the support structures are removed.

It has the capacity to build a volume of 1500 x 705 x 500 mm^3. An example of a dash part is shown in Figure 3.6. Renault's Formula 1 car is using only SLA and SLS models for their test in wind tunnel.

The unique part of SLA technology is its resolution and accuracy. Therefore, final product is very close to 3D drawing. By that way designer, engineers, sales managers and customers have opportunity see their products with all details and can accurately see error and shortcomings.

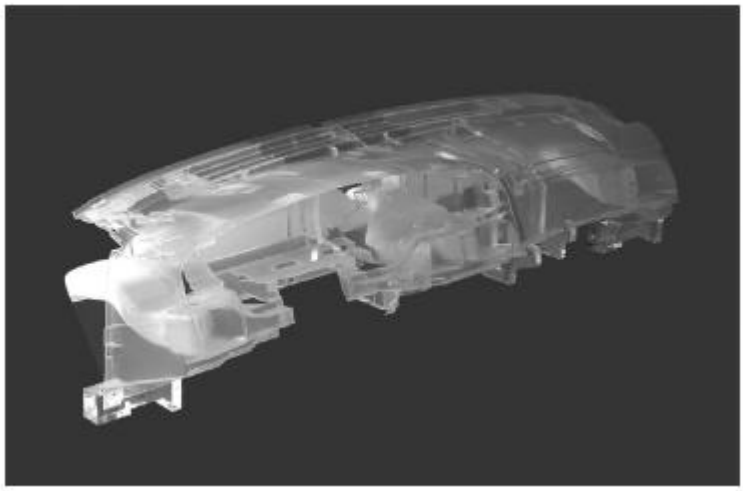

Figure 3.6 An SLA model of a dashboard part.

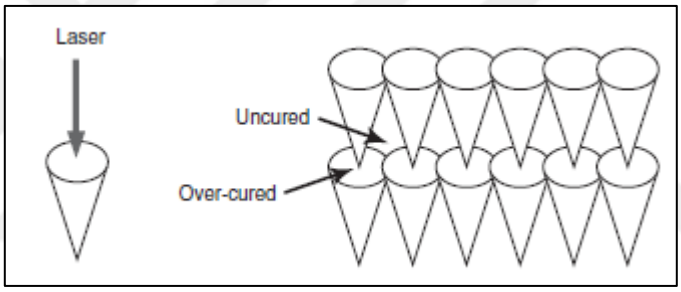

Figure 3.7 The cone features generated by the laser curing process resulting in uncured regions throughout the part.

Therefore real part can be made quickly and inexpensively, guaranteeing companies the best product possible, in the shortest time possible. This technology begins to use intensively in all kinds of industries such as aerospace, consumer electronics, automotive, military, surgical application, dental application and toys. This technology is the first of among 3D printers. Therefore SLA is regarded as benchmarks by other methods are judged. Early SLA methods have some problem such as being brittle and some warpage problem. However recent developments about SLS have largely corrected these problems.

It is very important for any 3D techniques to be very stable. SLA is a process that has the feature that being unattended building process. Once it started, the process goes full automatic and without any human intervene until process is completed. SLA process has also good dimensional accuracy with ±0,1 mm. Due to liquid properties this process

maintain perfect dimensional accuracy and glass like finish on the top surfaces part. But side walls may prominent surfaces as traces of additive manufacturing. 3D Systems Inc. have developed a software named as “QuickCast” for built parts with hollow interior which can directly as a wax pattern for investment casting. This might be good example of gradual development of SLA.

Despite its advantages SLA has some problems. Water absorption into resin over time in thin areas will result in curling and warping. On the other hand this system is relatively high compared to FDM and material is only photosensitive resin. SLA printed parts cannot be used for thermal and durability testing. Because energy is conducted in cone shape and during process some regions may be uncured as shown in Figure 3.7. The cost of resin and UV laser is quite expensive. Moreover optical sensor needs fine tuning in order maintain its optimal condition. After part is completed labors required to clean support structures and excess resin trapped in blind holes.

The major advantage of 3D printing processes can be used for all kinds of geometrical shapes with virtually no limitation. However liquid processes are one quite common problem. For instance, part with enclosed and hollow structures may trap liquid inside. Liquid can be drained in process or excess liquid may be discharged via hole. It still remains as a process limitation. The areas of application are restricted due to material limitation.

CHAPTER 4

COMPOSITE MATERIALS

4.1 Introduction

Composite material is used for material which have consists of at least two different phases with different properties. However composite materials have better properties than its contents. Most of the composite materials have one or more discontinuous phases (reinforcement) and these phases are distributed in one continuous phased (matrix). Discontinuous phases generally have better properties in order to improve discontinuous phases [40]. In this chapter classification of composite materials, polymer matrix composites and fabrication methods are explained.

4.2 Classification of Composite Materials

Composite materials are generally classified by their type of matrix material, their type of reinforcement material and geometry of reinforcement. Matrix materials are mostly classified as metal, ceramic or polymer materials [41]. In some other sources matrix materials are also classified as organic which refers polymer material, mineral which refers ceramic materials and metallic. Reinforcement phase's geometry mainly divided in to two classes as fiber and particle [40].

4.2.1 Polymer Matrix Composites

Polymer matrix composites (PMCs) have taken places as engineering materials. These polymer materials take places in engineering because of high performance reinforcement

materials such as glass, boron and aramid [41]. However it's not only reason PMCs take place in engineer. In recent times matrix materials have improved drastically. On the other glass fiber reinforced polymers represents still largest class in PMCs. Besides carbon fiber reinforced PMCs are used as structural component in aerospace field where strength and lightness are needed.

4.2.2 Metal Matrix Composites

Metal matrix composites (MMCs) have taken places as a material which uses matrix materials mostly aluminum magnesium and titanium [42]. These metals are reinforced with materials like silicon carbide and carbon based reinforcement in order to alter its properties. For example reinforcement of silicon carbide fibers can increase elastic modulus and tensile strength but cost of electrical conductivity. MMCs are mainly fabricated to have better properties than monolithic metals such as steel and aluminum alloys. MMCs have gain its unique properties with type of its reinforcement. They can be reinforced with low density metals such aluminum and titanium in order have high specific elastic modulus and tensile strength or can be reinforced with graphite which has low coefficient of thermal expansion in order to have tensile strength in high temperature. MMCs have a large field of application in military, aviation and transportation.

4.2.3 Ceramic Matrix Composites

Ceramic Matrix Composites (CMCs) are composites which have matrix material mineral based such as aluminum silicate. CMCs' advantages are high tensile strength, hardness, high service temperature due to ceramics, chemical resistance and low density. Despite of their good properties under impact or tensile stress they are damaged catastrophically. In order to overcome that very low toughness of ceramics, they are reinforced with silicon carbide and carbon. Under favor of these reinforcement CMCs have damage gradually instead of sudden and unexpected brittle fracture. These fiber and matrix combination makes ceramic materials more attractive to use by granting them better mechanical properties even in high service temperature. CMCs are mainly used in space technology and in cutting tools which has high service temperature.

4.3 Vat Photopolymerisation

In photopolymerisation process liquid resin which can be curable by UV light is a main material [38]. Actually most of the photopolymers react with UV lights but there are visible light systems are available. Upon contact with light materials undergo chemical reactions to solidify. This reaction is called as photopolymerisation.

Photopolymers were developed in 1960s soon after their development they found application area in in coating and printing industry. For example glossy papers are coated with photopolymers. In addition photopolymers are used in dentistry especially for filling top surface of filling in deep groves and prevent cavities. In these applications, coating cured by radiation that covers the resin without need of pattern either the material or the radiation. This application has changed with introduction of SLA.

Various type of radiation is used in order to cure commercial photopolymer such as gamma rays, X-rays, UV, electron beams or even visible lights. In vat polymerization (VP) commonly UV and visible light radiation are used. In microelectronics industry photomask materials are mainly photopolymer that cured by mostly UV lights and electron beams but in dentistry visible are used generally.

Two main configurations were developed for photopolymerisation processes in vat also there is one additional configuration has some research interest. Ink-jet systems are not counted among these processes due to its line-wise processing.

These processes are;

- Vector Scan (point wise), predominant type of commercial SLA machines
- Mask projection (layer wise), photopolymerisation of entire layer at one time
- Two-photon approaches, used for high resolution point-by-point approaches

These three type of configurations are shown in Figure 4.1 In vector scan and two-photo approaches scanning laser beams are needed but for mask projection large radiation beam that is patterned by different device, Digital Micromirror Device, are needed. In this thesis SLA type which uses Vector scan approach is used.

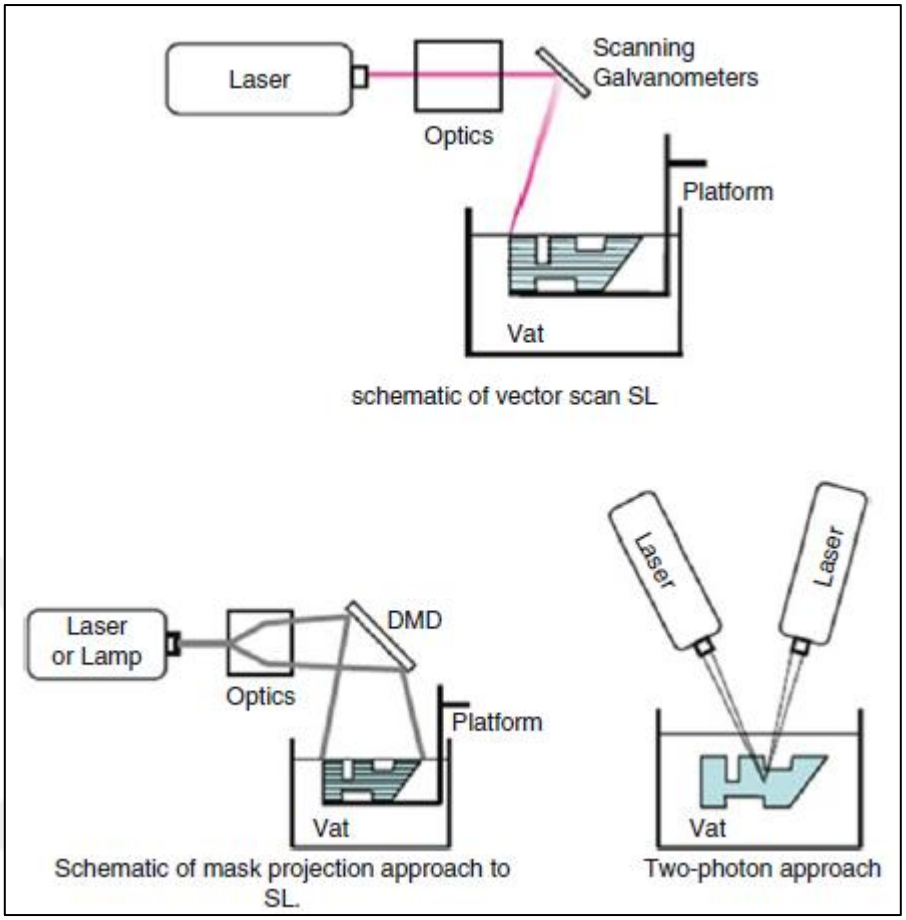

Figure 4.1 Schematic diagrams of three approaches to photopolymerisation processes [38]

4.4 Fabrication of Carbon Nanotube Reinforced Polymer Composites

Fabrication methods of CNT/polymer composites mainly focused on better and homogenous dispersion of CNTs in polymer matrix in order to have improved properties. The quality of nanotube dispersion in polymer matrix can be evaluated over range of length scales via imaging methods such optical microscopy, Scanning electron microscope (SEM), TEM and polarized Raman spectroscopy [43]. Recently confocal microscopy evaluates the nanotube dispersion in polystyrene/MWCNT composites [44]. Scattering method prove itself difficult to interpret because of low contrast. At local length scale, UV-vis near IR spectroscopy can determines nanotube dispersion state in in SWNT solutions and nanocomposite because of sharp peaks of individual or small bundles of SWNT. However

large bundles of SWNT give only monotonically decreasing absorbance with increasing wavelength [45].

CHAPTER 5

EXPERIMENTAL STUDIES

5.1 Introduction

In this chapter of the thesis, we scoped on the experimental study. In this part, scheme of the experimental study and used materials are introduced with their properties and related necessary data.

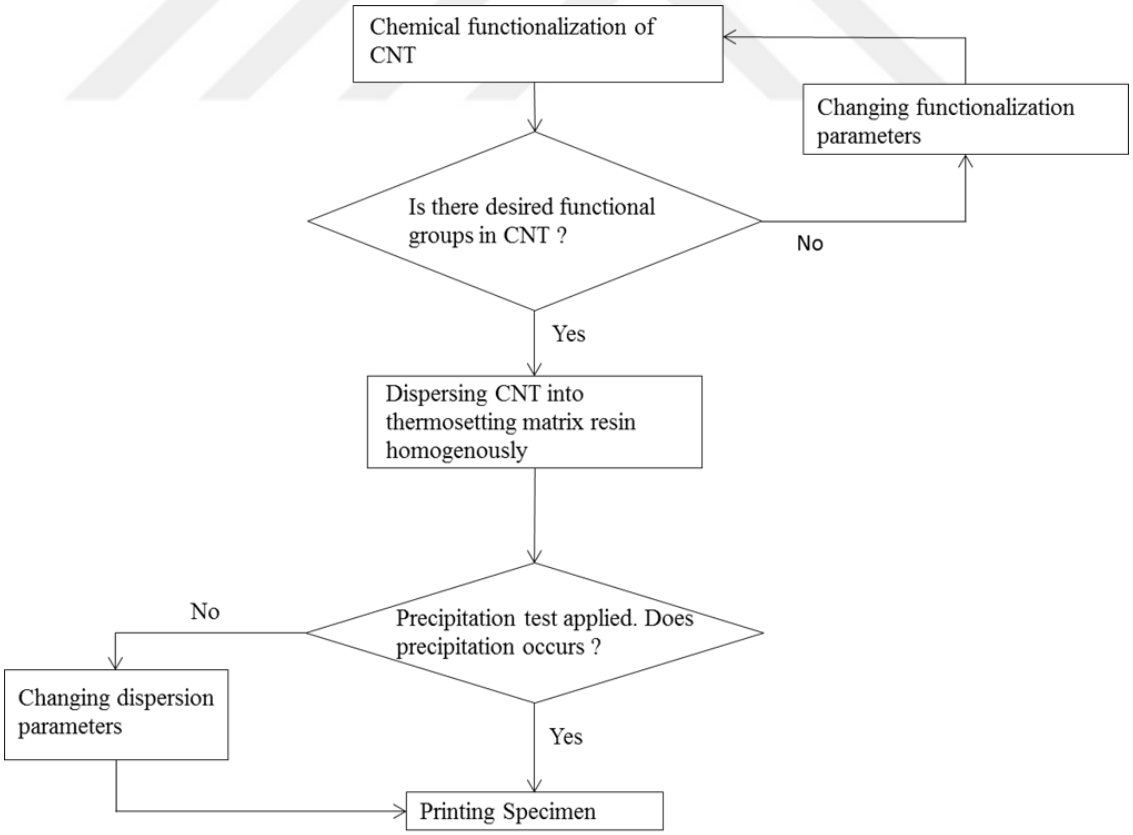

Figure 5.1 Scheme of experimental study

5.2 Materials and Tools

In this experiment, MWCNTs were purchased from Chengdu Organic Chemicals Co.Ltd., China. The specifications of MWCNTs are given in Table 5.1 and Table 5.2 [46].

Table 5.2 Specification of MWCNT

Purity	>%85
Outer Diameter	10–30 nm
Inner Diameter	5-10nm
Length	10-30 µm
Specific Surface Area	140 m^2/g
Tap Density	0,14 g/cm^3
True Density	2,1 g/cm^3
Electrical Conductivity	> 100 S/cm
Manufacturing Method	CVD

Table 5.1 Chemical analysis of CNT

Components	Contents (%)
C	88,33
Al	4,21
Fe	0,18
Ni	0,97
S	0,16

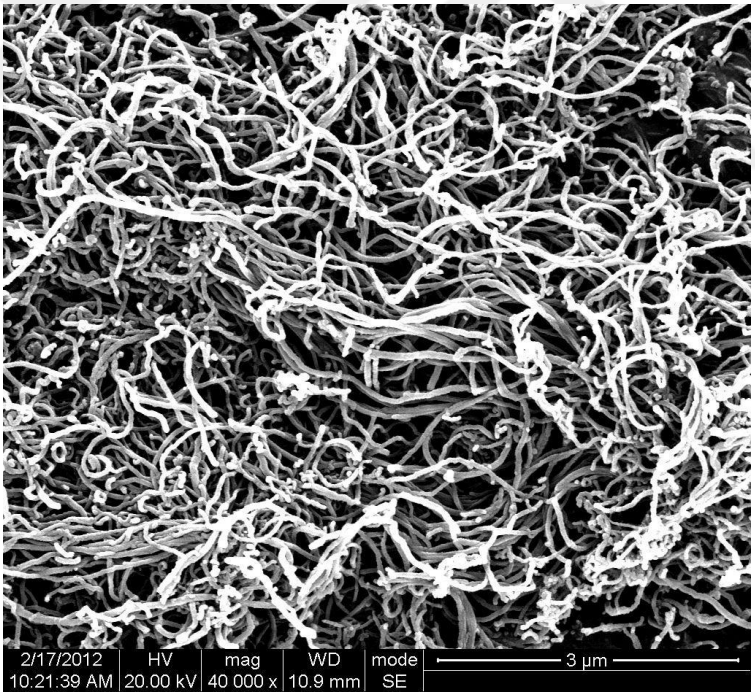

Figure 5.2 SEM image of MWCNT as received

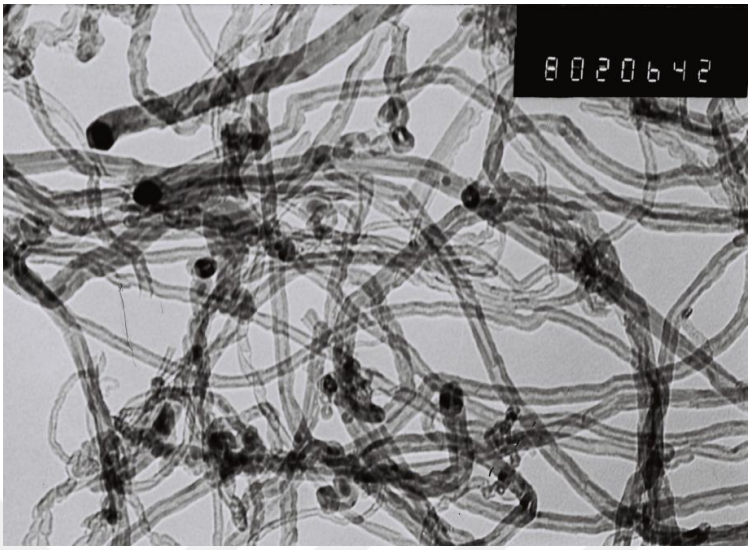

Figure 5.3 TEM image of MWCNT as received

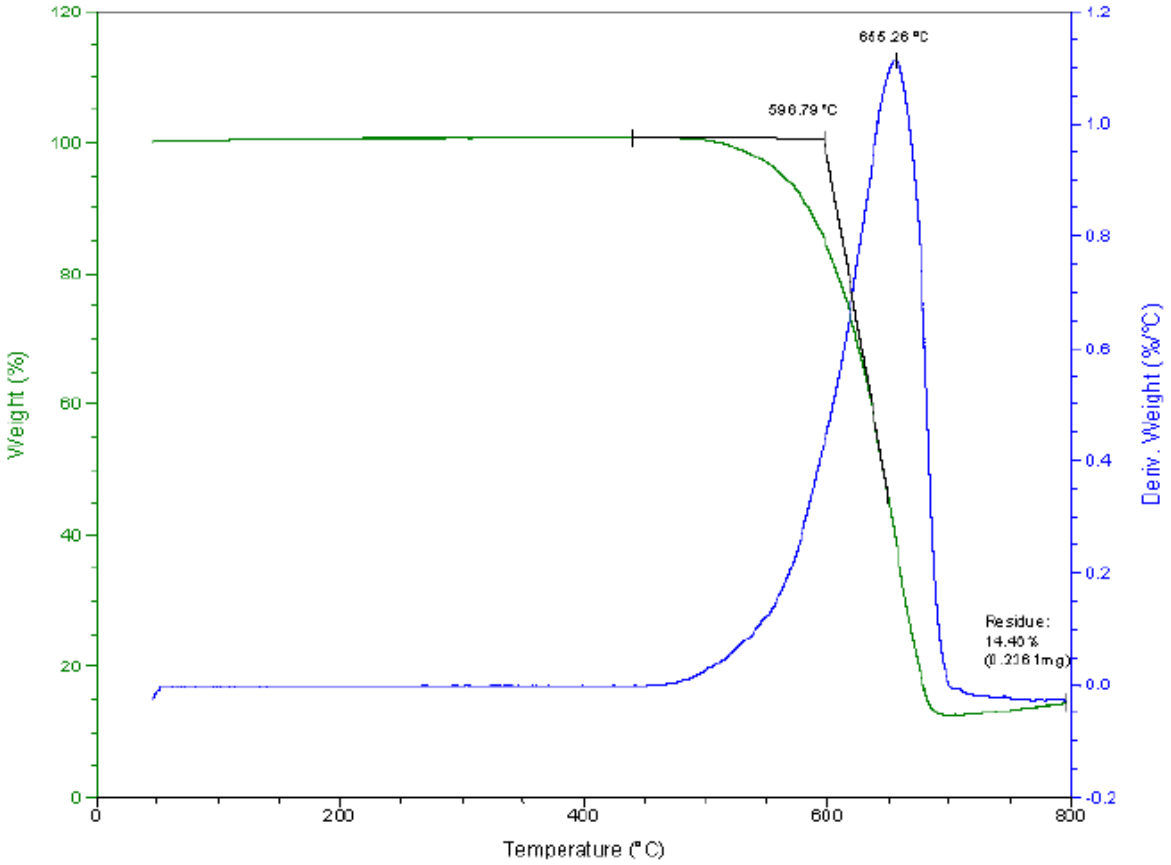

Figure 5.4 TGA/DTA analysis results of MWCNT as received

Photopolymer thermosetting resin was obtained from Formlabs, USA. In this experiment, we used standard gray resin. Specifications of the resin are given in Table 4.3 and Table 4.4.

Table 5.2 Properties of resin in solid phase

Tensile Strength	Elastic Modulus	Specific Weight	Strain Failure
38 MPa	1,6 GPa	1,09 – 1,12 gr/cm3	12 %

Table 5.3 Properties of resin in liquid phase

Viscosity	Boiling Point	Flash Point	Specific Weight
850 -950 cps (25°C)	> 100°C	>100°C	1,09 – 1,12 g/cm^3

5.3 Functionalization of Carbon Nanotubes

CNTs are known with its perfect mechanical and electrical properties. However, CNTs have serious agglomeration problems [47]. The reason is, pristine CNTs have no functional groups attached on the surface and tend to agglomerate with each other, because of Van der Waals bonds resulting from high specific surface area. If non-functionalized CNTs are used as reinforcement phase, it will cause much more agglomeration in polymer matrix [48]. Such defects and void effects owing to the agglomeration inside of the composite materials will dramatically decrease the mechanical properties of composites. Another problem associated with pristine CNTs in composites and blends is the lack of interfacial bonding which leads to fiber pullout under stress. Covalent functionalization can provide handle points for dispersion in host polymers; and also provide exfoliation of the bundles. In order to prevent undesirable effects, functionalization processes have to be applied.

Functionalization is a process that aims inserting functional groups on the sidewall of CNTs [49]. In order to insert functional groups between carbon molecules, we should break some bonds between carbon molecules. Due to those broken bonds, properties of CNTs will decrease.

In order to functionalize CNTs, there are several methods. These methods are mainly wet chemical methods, photo oxidation, oxygen plasma and gas phase treatment. In this experimental study, wet chemical functionalization was used. Literature screening shows that nitric acid is extensively used in order to functionalize MWCNT due to its strong oxidizing feature. Nitric acid functionalization produces mainly carboxyl groups but also produce hydroxyl and carbonyl groups as well, [50] which also increase solubilization of the nanotubes [51]. The process parameters for chemical reaction differs broadly such as acid concentration, amount of CNT and process duration.

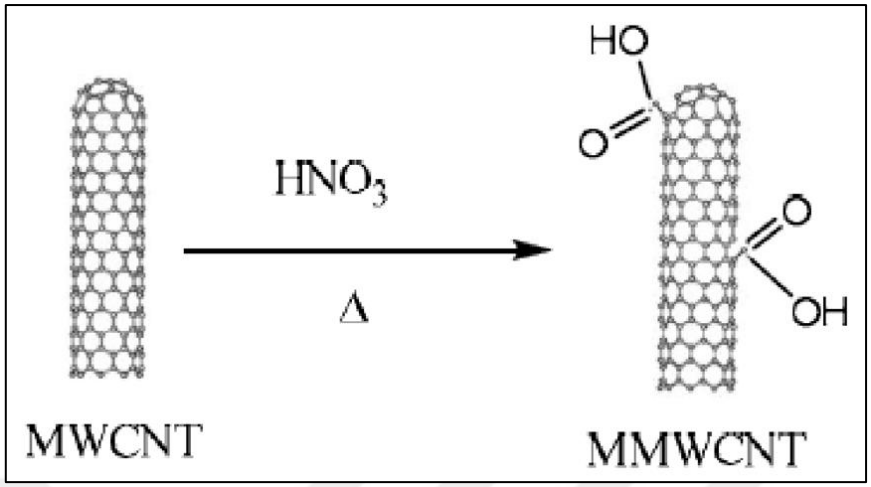

Figure 5.5 Chemically functionalization of CNT [52]

In this experimental study, nitric acid (65 wt%) was used for chemical functionalization. In this process, pristine CNTs were measured by precision scales and put into the flask; then 20 mL nitric acid solution added for each 0,1 gr CNTs. Mixture was gently shaken by hand in order to clean CNTs that stuck on the sidewall of flask. Mixture was put into the ultrasonic bath and sonicated for 2 hours. At the end of this process, it was expected that agglomerated CNT were dispersed in the solution homogenously.

Figure 5.6 Sonication of CNT in ultrasonic bath

Figure 5.7 CNTs after sonication

After sonication was completed, solution was stirred by magnetic stirrer at ~125°C in 600 rpm for 48 hours under reflux system. At the end of the process, solution was diluted by distilled water about six times of its volume. Diluted solution filtered by filtration system. In filtration system, PTFE filter with 0,45µm pore size was used in order to separate CNTs from solutions. Separated CNTs were washed with distilled water and filtered until they reached the neutral pH. CNTs were dried at 40°C in the air furnace overnight (about 18 hours) and at 100°C for 2 hours. Dried CNTs are held in desiccator until we use them for resin preparation process in polymer matrix.

Figure 5.8 Reflux system

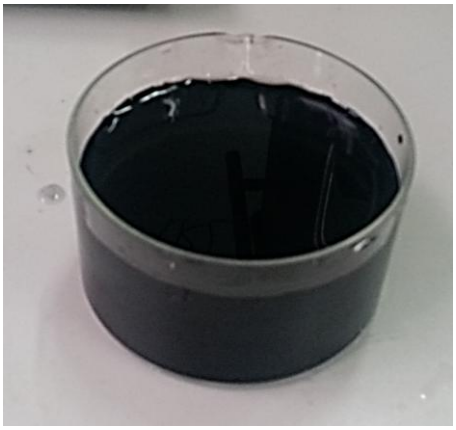

Figure 5.9 Diluted CNT mixture

Figure 5.10 Filtration system

In order to identify functional groups created by functionalization process, FT-IR tests were applied both functionalized and pristine CNTs. FT-IR Spectroscopy analysis was performed by Spectrum 100 (Perkin Elmer, Germany) which has an operating range between 650 cm^{-1} to 4000 cm^{-1}.

Figure 5.11 Perkin Elmer Spectrum 100

The FT-IR result of pristine CNTs given in Figure 5.12 shows that there are no functional groups attached on the surface of CNTs. There are peak points around 2000 cm^{-1} that indicate there are C=C bonds inside the CNT.

The FT-IR result of functionalized CNTs is shown in Figure 5.13. It can be clearly seen from the FT-IR results, there are various peak points indicating the functional groups on the surface of CNTs. Broad peaks between 3000 cm^{-1} and -2500 cm^{-1} are related to the O-H bonds. It indicates us that we have hydroxyl groups that attached to carboxyl or carbonyl groups. Also there are two distinct peaks in 2321,67 cm^{-1} and 2087,41 cm^{-1}, which indicates C≡C bending of the multi-wall carbon nanotube after the formation of defects. In 1808,74 cm^{-1} and 1669,92 cm^{-1}, there are also two distinct peak points. These peaks are related with amides C=O bonds which are functional groups called as carbonyl. Peak points in 1538,93 cm^{-1} stretching shows us we have C=C bonds, this peak shows, there are carbon atoms without any defect in CNT. In fingerprint region, there is one peak in 1402,71 cm^{-1} stretching refers to strong aromatic C-H group that effects electrical properties. The last peak 1077,87 cm^{-1} stretching indicates us C-O functional group that is the product of oxidation of carbons. All these functional groups are shown in Table 4.5.

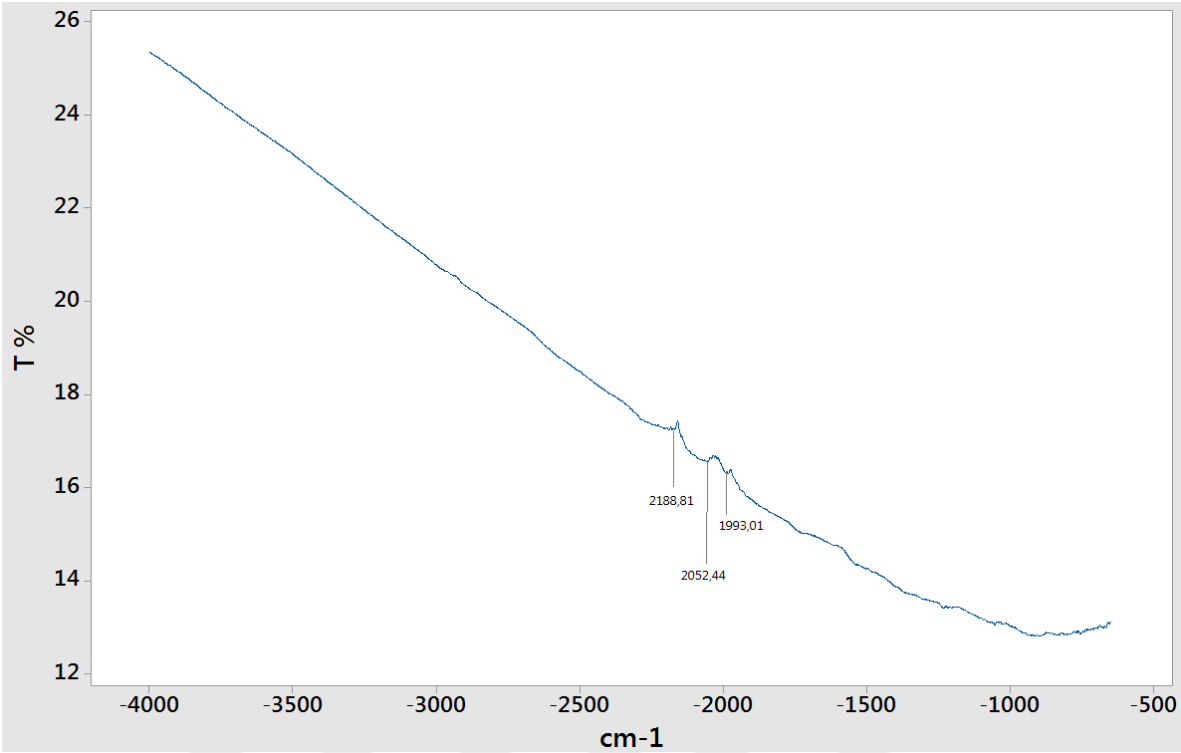

Figure 5.12 FT-IR result of pristine CNT.

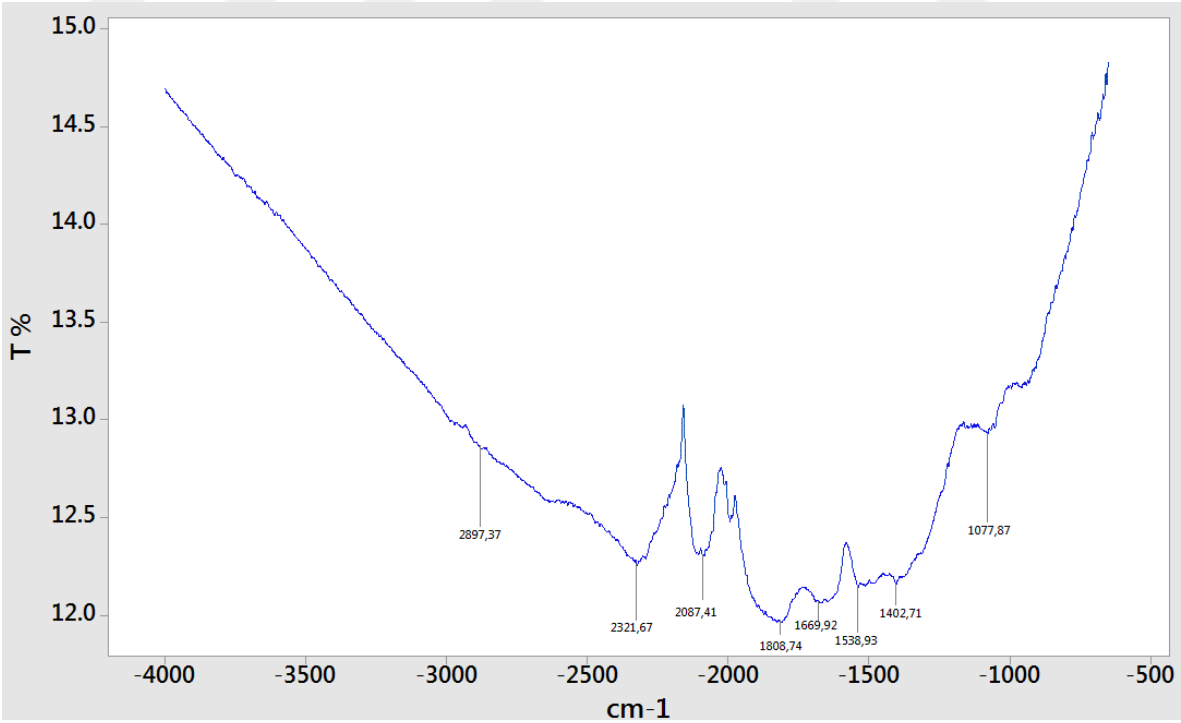

Figure 5.13 FT-IR result of functionalized CNT

Table 5.4 Identified functional groups in CNT

1077,87 cm^{-1}	C-O
1402,71 cm^{-1}	C-H
1538,93 cm^{-1}	C=C
1669,92 cm^{-1}	C=O
1808,74 cm^{-1}	C=O
2087,41 cm^{-1}	C≡C
2321,67 cm^{-1}	C≡C
2963,30 cm^{-1}	O-H

We desired to have carboxyl, carbonyl and hydroxide groups on CNTs in order to accept our chemical functionalization process was carried out successfully. As a result of FT-IR test, we identified that we have –OH groups that indicates hydroxyls, -OH and C=O groups that indicates carboxyls and C=O groups that indicate carbonyls. As we obtained the desired groups on CNTs, we are ready to proceed the resin preparation process.

5.4 Preparation of Nano Composite Resin and Sedimentation Test

As we aspire to produce nanocomposite resin for SLA type 3D printer, this fluid should have colloidal stability since resin may not be intended to be used just after its preparation. Therefore, prepared nano suspensions should have colloidal stability for reasonable amount of time. In order to meet this requirement we focused on the preparation of nano suspension and sedimentation test to verify its stability in this section.

In literature two kinds of method exist; one-step method and two-step method. In one step-method production of particles and synthesis of nano suspension are done simultaneously. This method is not so popular as literature show us. Because in this method particles

created in the system is not CNTs but carbon flakes [53]. In two-step method, CNTs are produced first, and then it is dispersed in the base fluid. It is the most popular method to produce CNT based nano suspension [54].

For measuring the stability of nano suspension there are several methods and tools. One of them is visual inspection in static conditions for some period of time [55]. Apart from visual inspection there are some quantitative methods. Among these methods measuring zeta potential is one the most popular method. Zeta potential is degree of adjacent charged particle of functional group and the base fluid. Measured value can be either positive or negative, important point in zeta potential's absolute value. Higher value means better stability and zero means cannot be ensured. Zeta potential can also be measured by change of pH. Since, pH is directly related to electrostatic charge on particles' surface.

In this experimental study, stability was observed by macro visual observation method. Owing to the opaque property of our resin we were not able to use quantitative methods. After nanocomposite resin is prepared, resin is visually observed periodically. In experiment, one month of stability is objected.

In experiments, we produced nanocomposite resin in four different reinforcement ratios as 0,25 wt%, 0,50 wt%, 0,75 wt% and 1 wt%. For production pure resin and selected amount of CNT was mixed and stirred with a stick in tube. After resin is mixed with stick superficially, mixture was put into ultrasonic bath and sonicated for 2h. If nanocomposite resin did not disperse homogenously due to higher rate of reinforcement, sonication time increased until visual observation shows us that homogenous dispersion is ensured.

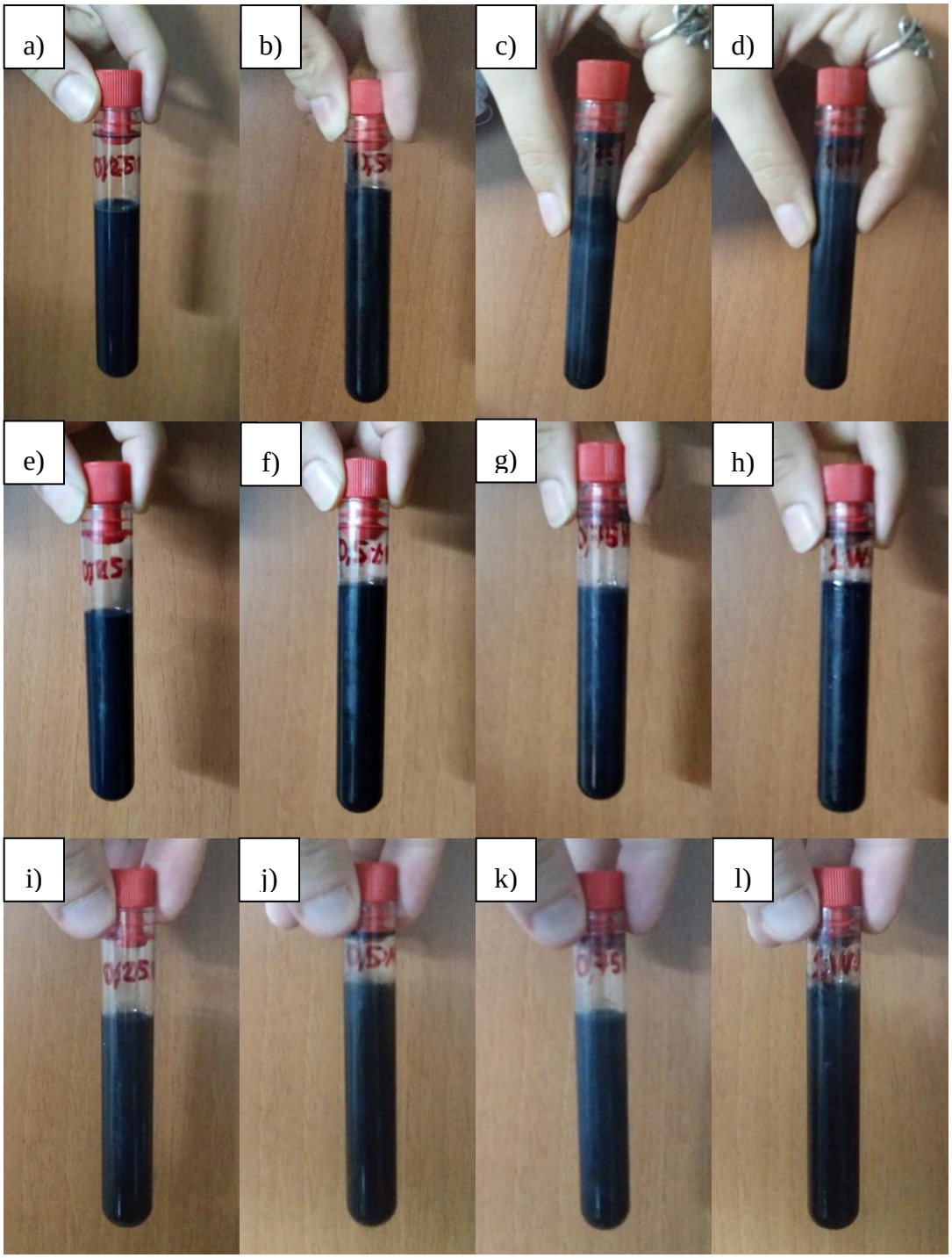

Figure 5.14 Sedimentation test images of CNT in resin. Resin with (a) 0,25 wt% (b) 0,5 wt% (c) 0,75 wt% and (d)1 wt% CNT ratios right after homogenous dispersion. Resin with (e) 0,25 wt% (f) 0,5 wt% (g) 0,75 wt% and (h)1 wt% CNT ratios 24 hours later after homogenous dispersion. Resin with (i) 0,25 wt% (j) 0,5 wt% (k) 0,75 wt% and (l) 1 wt% CNT ratios a week later after homogenous dispersion.

5.5 Printing Nanocomposite

We manufactured CNT reinforced polymer matrix nanocomposite material specimens subsequent to the preparation of nano suspensions. In this study, our nanocomposite specimens were printed by Formlabs 2+ SLA type 3d printer (Formlabs Inc., USA).

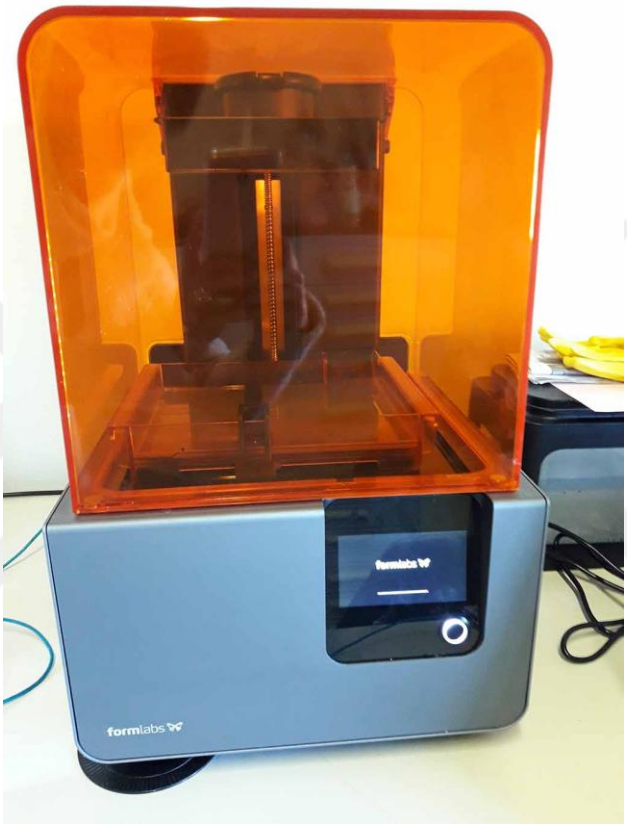

Figure 5.15 Formlabs 2+ SLA type 3D Printer

Before printing our specimens, we need to add support structures on our specimens, otherwise printing will be impossible due to the lack of surfaces. In order to create that support structures we used the software entitled Preform (Formlabs Inc., USA) to make our specimen ready for printing. It is possible to print the specimen in any orientation. We chose our base surface as largest surface and we oriented tensile specimens parallel to the base surface with a 90˚ orientation of largest surface of specimens to the base surface. Also, wear specimens are oriented by 0˚ to the ground as shown in Figure 5.16.

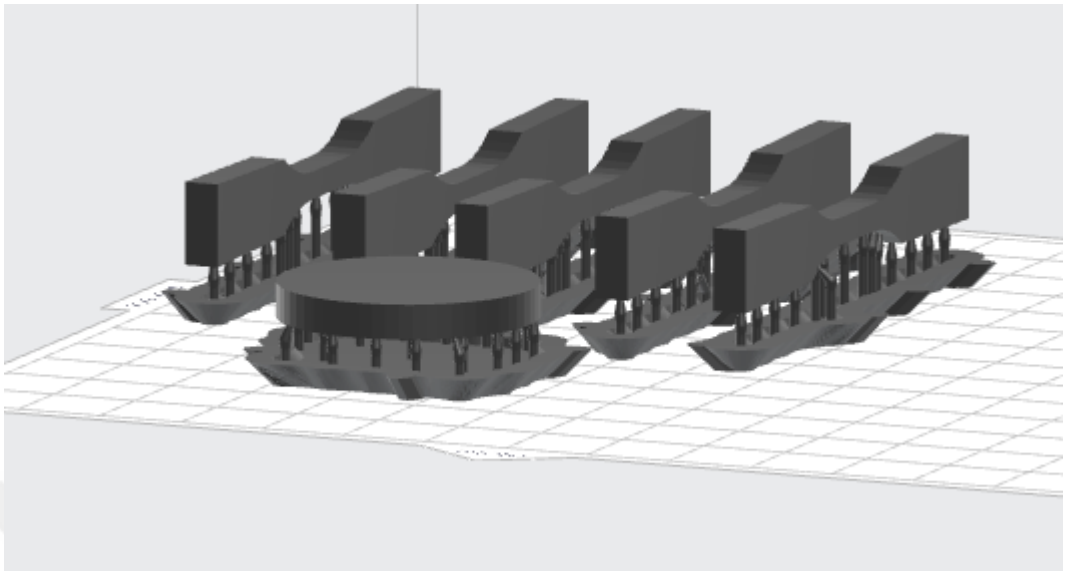

Figure 5.16 Specimens with support structures.

In our first trial we aimed to manufacture specimens from our first nano suspension which has 0,25 wt% CNT ratio. However, at the end of our printing process we failed at the manufacturing of composites. The reason of failure is related to the high level UV absorption of CNTs in composite nano suspension which inhibits the reaction of photopolymer [56] just like other carbon based materials. As an initial and immediate solution, we decreased the CNT ratio to 0.02 wt%, because light source of our 3D printers cannot be adjusted in means of energy increment.

5.6 Mechanical Tests

5.6.1 Tensile Test

In this test, we aim to determine the tensile strength of base (unreinforced) and CNT reinforced specimens. In this test, we use a class 1 calibrated electro-mechanic testing device (modernized by ALŞA Material Testing, Turkey) (Figure 5.17). We determined specimen dimension according to D638-14 Standard Test Method for Tensile Properties of Plastics [57]. We printed our specimens in dog bone shape according to this standard for both base and composite specimens and used them in tensile tests as fabricated. These two specimens are shown in Figure 5.18.

Figure 5.17 Electro-mechanical Testing Device used for Tensile Tests

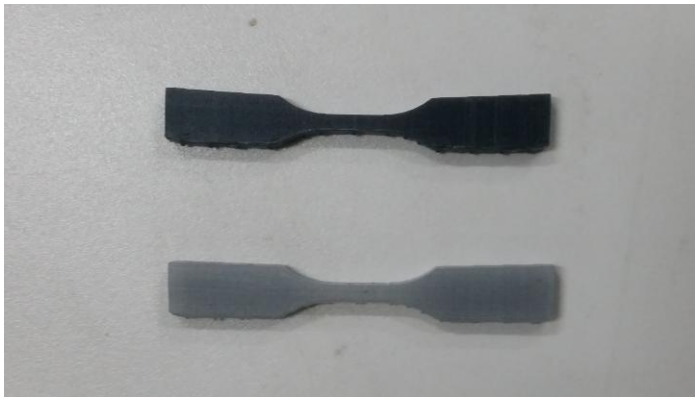

Figure 5.18 Tensile Test Specimens

5.6.2 Wear Test

In this test, we aim to define wear rate, specific wear rate and friction coefficient of base and CNT reinforced composite specimens. We tested our wear test specimens by using a Ball-on-Disk (Pin-on-Disk) Tribotester (TRIBOtechnic, France) (Figure 5.19). We

determined specimen dimensions according to ASTM G99-05 Standard Test Method for Wear Testing with a Pin-on-Disk Apparatus [58]. According to this standard disc specimens for both base and CNT reinforced composite materials are prepared. These specimens' that shown in Figure 5.20 and Figure 5.21 are 30 mm in diameters and 4 mm in thickness. Tests are applied on each specimen in 2, 4, 6, 8, 10 and 12 mm radius. In 2, 6 and 10 mm radii system run according to 40000 cycles so distances are defined for 40000 cycles. In 4, 8 and 12mm radii system run according to 500 m distance. Also force is applied in 10 N in order to calculate specified wear rate. In this test abrasive ball material is Ø6mm 100Cr6 cold work tool steel.

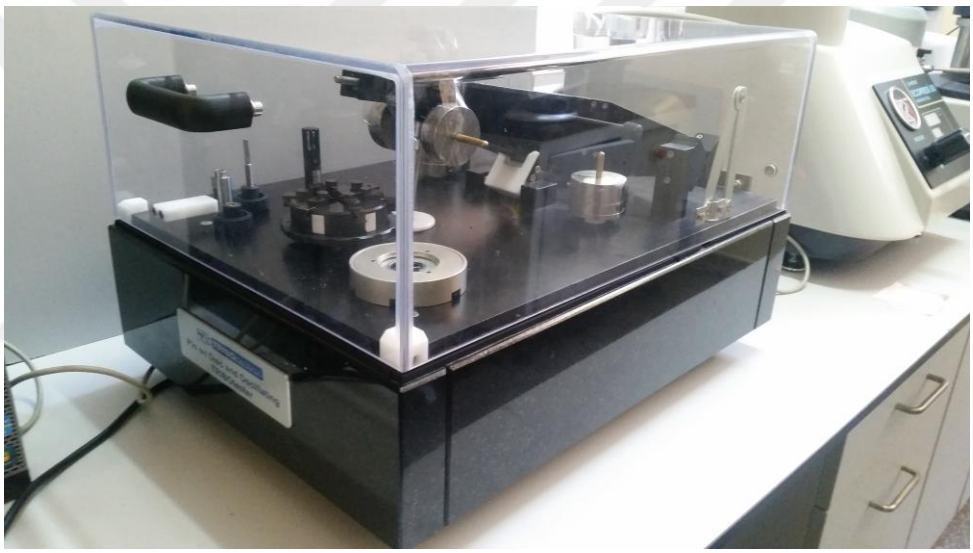

Figure 5.19 Tribotechnic Pin-on-Disk Tribotester

Figure 5.20 Disc type wear test specimen of base material

Figure 5.21 Disc type wear test specimen of CNT reinforced composite material

In this test, volume losses were defined by the measurement of wear track on the disk specimens. Wear track widths were measured by a stereo macroscope (AOB lab) (Figure 5.22). Volume losses are calculated by using the following equation:

$$Volume\ loss = (\arcsin\left(\frac{a}{2r_{ball}}\right).r_{ball}^2 - \frac{a}{2}.\sqrt{(r_{ball}^2 - \frac{a^2}{4})}).2.\pi.r_{wear} \quad (5.1)$$

where, a is the measured width of track, r_{ball} is the pin end radius (3 mm), r_{wear} is wear track radius that created on specimen.

Figure 5.22 Macroscope

In order to calculate wear rate and specified wear rate we need both volume loss and test running distance. Equation 5.2 shows how to define wear rate. Moreover, specified wear rate which is also function of load is defined by Equation 5.3

$$Wear\ Rate = Volume\ loss\ \times\ Run\ Distance \tag{5.2}$$

$$Specified\ Wear\ Rate = Wear\ Rate\ \times Load \tag{5.3}$$

5.6.3 Results and Discussion

3D printed products have limited range of use due to their lower mechanical properties owing to the effects of additive manufacturing. However, we have prepared functionalized MWCNTs and reinforced SLA type resin with those functionalized MWCNTs. We manufactured specimens for tensile and wear test to see how much MWCNTs effect the mechanical properties. However, during our printing process we realized that higher CNT reinforcement ratio gives rise to absorption of UV light and printing becomes impossible with our existing 3D printers. Therefore, a lower reinforcement ratio was chosen.

According to the standards, we applied tensile tests using five specimens for each type of materials, average results of these five specimens are calculated as the tensile strength of specimens and all result are listed in Table 5.5. Moreover, tensile test results are given in Appendix A.

Table 5.5 Tensile Test Results

Test Number	Base Specimen Tensile Strength (MPa)	Reinforced Specimen Tensile Strength (MPa)
1	33.92	57.87
2	39.90	64.85
3	30.18	69.33
4	41.16	64.60
5	42.65	66.10
Average Result with Standard Deviation	37.56 ±5.29	64.55 ±4.18

According to the tensile test result we can explicitly indicate that we enhanced the average tensile strength of 3D printed materials over 70%. Despite our quite low (0,02 wt%) CNT reinforcement ratio the tensile strength is improved dramatically. We can expect that result because MWCNT has far superior tensile strength than solid phase of resin. The industrial catalog [59] indicate that the solid phase of cured resin has a tensile strength about 38MPa just as we measured. However, theoretical tensile strength of MWCNT's are nearly 300 GPa and the effective strength of our nanotubes seem to be over 150GPa; therefore, our reinforced specimens introduce superior tensile strength than base specimens [60].

As we examine fracture surface of tensile specimens, we can clearly see distinction between two different types of specimens. We can see quite textured area on the fracture surface. Such fracture surfaces can be attributed to brittle fractures [61]. As the roughness of the fracture surface becomes intensive, it shows us that more strain energy is absorbed during the fracture process.

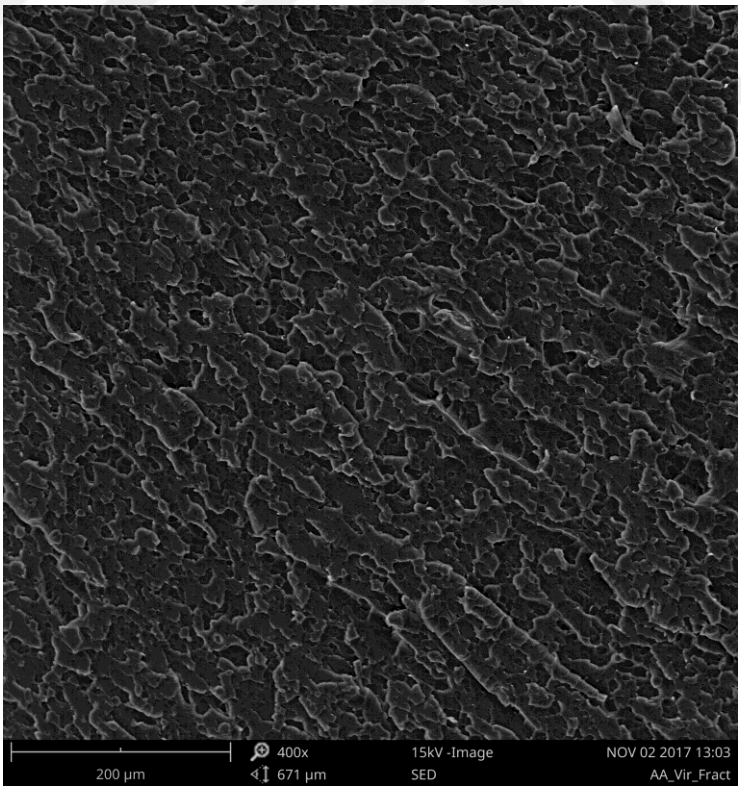

Figure 5.23 SEM Images of base tensile test specimen surface

We observe quite rough fracture surface from CNT reinforced tensile test specimen. We can explicitly see that surface has no continuous fracture phase. There are interruptions like voids and pores on the fracture surface; those interruption shows us that strain energy is absorbed during fracture. Moreover, CNTs have strengthening mechanism that increases tensile strength; one of these mechanisms is dispersion strengthening due to nano size of MWCNTs [62]. Also it is known that interface between CNT and matrix are related with mechanical properties of nano composite [63]. As we consider bridging and pulling out manner, the interface strength between CNTs and polymer matrix and fracture energy of the composites are going to increase [64]. On the other hands CNTs are nano materials with smaller cross sections; so during fracture occurs, CNTs can arrest smaller crack tips [65]. By this way, energy of cracks dissipates into two different cracks. This mechanism slows down the crack propagation on fracture surface. In our study this mechanism occurs even in smaller scale. This cracking mechanism leads into moderate fracture surface roughness as we can see from our fracture surface. Another of Perez et al. [66] study shows us that FDM printed specimens have some gaps on fracture surfaces.. These gaps are results of additive manufacturing with FDM type printers. In our study both types of specimens have no visible gaps between layers, this condition increases tensile strength of our specimen even more. Therefore, we understand that SLA type printed nano composites are even more promising than FDM printed nano composites.

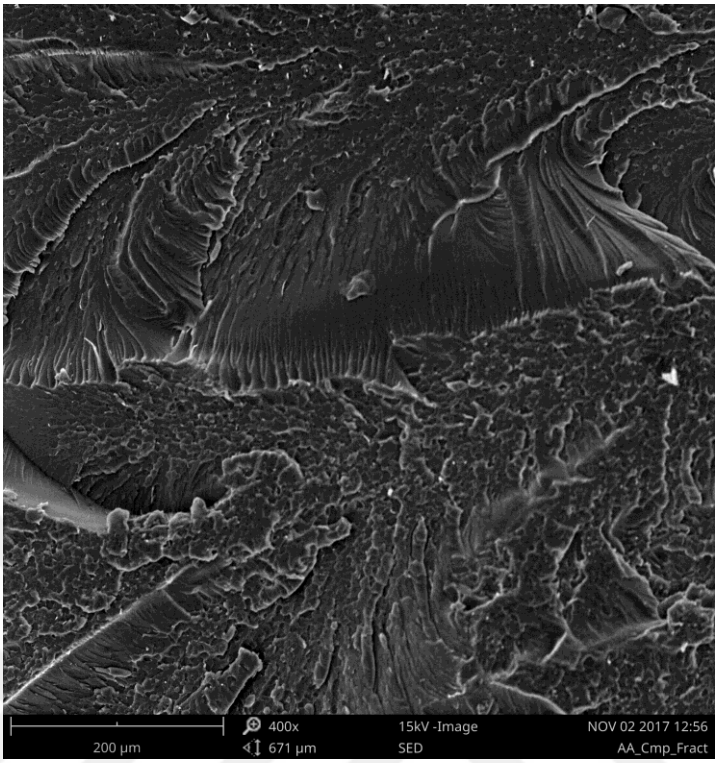

Figure 5.24 SEM Images of reinforced tensile test specimen surface

Table 5.6 Calculated Wear Rate and Specified Wear Rate of Base Specimen

Radius (mm)	Run Distance (m)	Wear Rate (mm^3/m)	Specified Wear Rate ($mm^3/m.N$)
2	503	$22,774519*10^{-3}$	$22,774519*10^{-4}$
4	500	$18,600959*10^{-3}$	$18,600959**10^{-4}$
6	1509	$31,615815*10^{-3}$	$31,615815*10^{-4}$
8	500	$1,384407*10^{-3}$	$1,384407*10^{-4}$
10	2514	$0,401972*10^{-3}$	$0,401972*10^{-4}$
12	500	$2,278693*10^{-3}$	$2,278693*10^{-4}$

Table 5.7 Calculated Wear Rate and Specified Wear Rate of Reinforced Specimen

Radius (mm)	Run Distance (m)	Wear Rate (mm^3/m)	Specified Wear Rate ($mm^3/m.N$)
2	503	$9,976448*10^{-3}$	$9,976448*10^{-4}$
4	500	$0,703736*10^{-3}$	$0,703736*10^{-4}$
6	1509	$0,416579*10^{-3}$	$0,416579*10^{-4}$
8	500	$1,038642*10^{-3}$	$1,038642*10^{-4}$
10	2514	$0,262951*10^{-3}$	$0,262951*10^{-4}$
12	500	$0,405738*10^{-3}$	$0,405738*10^{-4}$

As these results show us that CNT reinforced composite specimen has much better results in both wear rate and specified wear rate than base specimen. Specified wear rate is improved up to 98 percent. It shows us that CNT increases specified wear rate dramatically

Table 5.8 Friction coefficients of specimen

Radius	Base	Reinforced
2	0,395	0,225
4	0,357	0,093
6	0,389	0,089
8	0,098	0,095
10	0,102	0,110
12	0,097	0,083

Also it is expected that CNT may improve friction coefficient as well as specified wear rate. Our tribotester machine measures average friction coefficient. So we may see difference between base and reinforced specimen in Table 5.8. Also all wear test graphs are given in in Appendix A.

In our wear tests, we determined specified wear rate and friction coefficient. Results show us that we also have improvement in friction coefficients up to 77 percent. In previous similar properties with lower percentages (~10%) have obtained in specific wear rate and friction coefficient [67]. In our studies we have similar results with 3D printed nanocomposite specimens as well. Since MWCNTs have a minimal van der Waals interaction between their walls and each other [68]. Each layer of MWCNT slides from each other nearly frictionless. Therefore, MWCNTs behave as nano ball bearings and as a lubricating agent which is a property of layered carbon allotropes.

In order to understand wear type on specimens, we examine wear surface to see which type of mechanism is effective on surfaces. We observe voids and particles that stuck in surfaces

on base specimen. These signs show us that abrasive wear is effective on surface. (Figure 5.25) However, adhesive wear helps the surface to close the wear tracks of abrasive wear on the surface. In addition abrasive particles may cause higher friction coefficient [69].

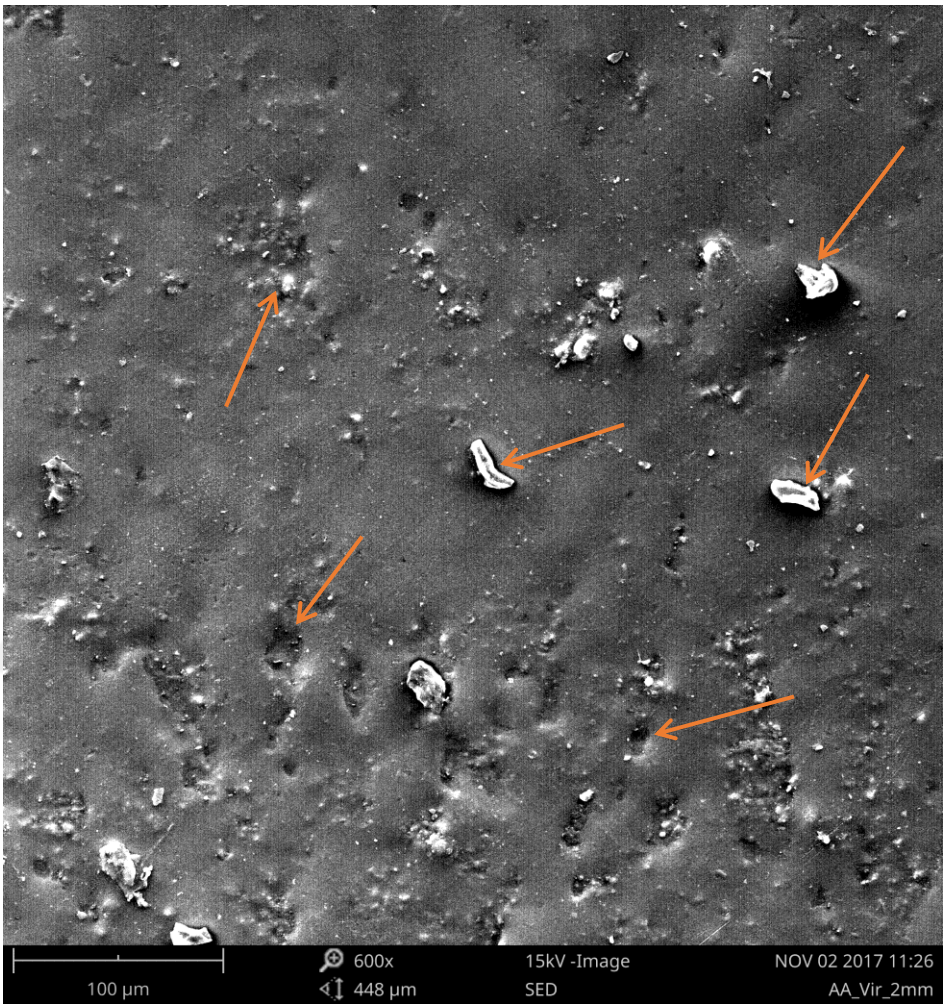

Figure 5.25 SEM Image of base test specimen

As we examine the surfaces of the reinforced wear test specimen's, we can see layer on layer structure (Figure 5.26). This formation gives us the idea of adhesive wear formation on the surface. This layer on layer structure is even more distinctive between wear and normal surfaces. Besides, we can see particles and hollows as well. However, the CNT reinforced specimen has fewer particles and hollows than the base specimen. Therefore, this situation may also explain lower friction coefficient of reinforced specimens as well as minimal van der Waals interaction between MWCNTs.

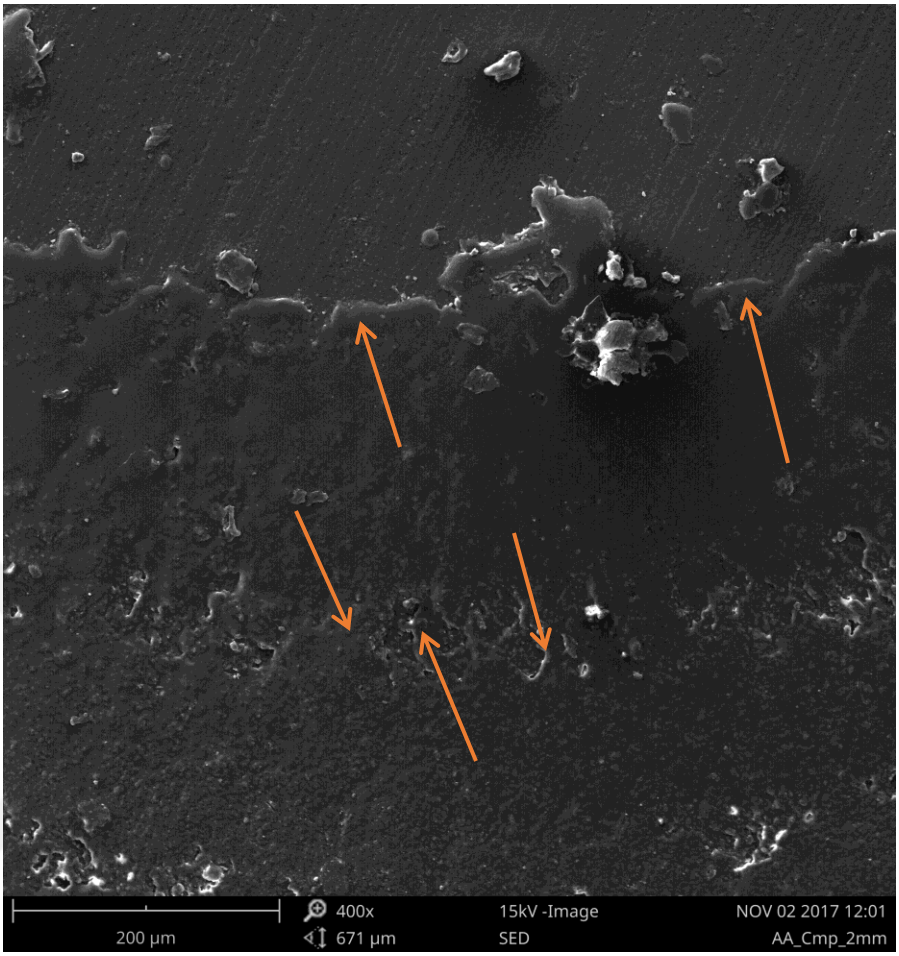

Figure 5.26 SEM Image of base test specimen

CHAPTER 6

CONCLUSION

1. As a result of our process, MWCNTs are successfully functionalized and homogenously dispersed in base resin. Sedimentation test proves that short and long term of stability of resin is provided properly.

2. In printing process, we clearly understand that CNTs' UV absorption may affect printing process negatively. Therefore, in order to complete printing successfully, UV light parameters or CNT ratio of nano composite resin should be optimized adequately.

3. Tensile properties of the resin material are improved up about 70% even with 0,02 wt% CNT reinforcement.

4. Wear properties of the resin material are increased up about 98% and friction coefficient of material is improved up about 77%.

In conclusion, we have great enhancement on the mechanical properties of resin material. This study shows us that even with very low ratio of MWCNT reinforcement can highly improve the quality of 3D printed product. In the future, we believe that our recent problem will be over by the applications of nano composite materials. As one of the most important problems about the 3D printed products solved, 3 dimensional printings can find itself more application fields

REFERENCES

[1] Iijima, S., (1991). "Helical microtubules of graphitic carbon", Nature, 354: 56.

[2] Sun, Y.-P. Fu, K. Lin, Y. and Huang, W., (2002). "Functionalized Carbon Nanotubes: Properties and Applications", Accounts of Chemical Research, 35: 1096-1104.

[3] Dalton, A.B. Collins, S. Munoz, E. Razal, J.M. Ebron, V.H. Ferraris, J.P. Coleman, J.N. Kim, B.G. and Baughman, R.H., (2003). "Super-tough carbon-nanotube fibres", Nature, 423: 703-703.

[4] Sandler, J.K.W. Kirk, J.E. Kinloch, I.A. Shaffer, M.S.P. and Windle, A.H., (2003). "Ultra-low electrical percolation threshold in carbon-nanotube-epoxy composites", Polymer, 44: 5893-5899.

[5] Qian, D. Wagner, G.J. Liu, W.K. Yu, M.-F. and Ruoff, R.S., (2002). "Mechanics of carbon nanotubes", Applied mechanics reviews, 55: 495-533.

[6] Schadler, L. Giannaris, S. and Ajayan, P., (1998). "Load transfer in carbon nanotube epoxy composites", Applied physics letters, 73: 3842-3844.

[7] Zhu, J. Peng, H. Rodriguez-Macias, F. Margrave, J.L. Khabashesku, V.N. Imam, A.M. Lozano, K. and Barrera, E.V., (2004). "Reinforcing epoxy polymer composites through covalent integration of functionalized nanotubes", Advanced Functional Materials, 14: 643-648.

[8] Shieh, Y.-T. Wu, H.-M. Twu, Y.-K. and Chung, Y.-C., (2010). "An investigation on dispersion of carbon nanotubes in chitosan aqueous solutions", Colloid and Polymer Science, 288: 377-385.

[9] Hull, C.W., (1986). Apparatus for production of three-dimensional objects by stereolithography, Google Patents.

[10] Zhong, W. Li, F. Zhang, Z. Song, L. and Li, Z., (2001). "Short fiber reinforced composites for fused deposition modeling", Materials Science and Engineering: A, 301: 125-130.

[11] Tekinalp, H.L. Kunc, V. Velez-Garcia, G.M. Duty, C.E. Love, L.J. Naskar, A.K. Blue, C.A. and Ozcan, S., (2014). "Highly oriented carbon fiber–polymer composites via additive manufacturing", Composites Science and Technology, 105: 144-150.

[12] Klift, F.V.D. Koga, Y. Todoroki, A. Ueda, M. Hirano, Y. and Matsuzaki, R., (2016). "3D Printing of Continuous Carbon Fibre Reinforced Thermo-Plastic (CFRTP) Tensile Test Specimens", Open Journal of Composite Materials, Vol.06No.01: 10.

[13] Matsuzaki, R. Ueda, M. Namiki, M. Jeong, T.-K. Asahara, H. Horiguchi, K. Nakamura, T. Todoroki, A. and Hirano, Y., (2016). "Three-dimensional printing of continuous-fiber composites by in-nozzle impregnation", Scientific Reports, 6: 23058.

[14] Dul, S. Fambri, L. and Pegoretti, A., (2016). "Fused deposition modelling with ABS–graphene nanocomposites", Composites Part A: Applied Science and Manufacturing, 85: 181-191.

[15] Lin, D. Jin, S. Zhang, F. Wang, C. Wang, Y. Zhou, C. and Cheng, G.J., (2015). "3D stereolithography printing of graphene oxide reinforced complex architectures", Nanotechnology, 26: 434003.

[16] Tsiakatouras, G. Tsellou, E. and Stergiou, C., "Comparative study on nanotubes reinforced with carbon filaments for the 3D printing of mechanical parts".

[17] Hector Sandoval, J. and Wicker, R.B., (2006). "Functionalizing stereolithography resins: effects of dispersed multi-walled carbon nanotubes on physical properties", Rapid Prototyping Journal, 12: 292-303.

[18] Haddon, R.C. and Chow, S.Y., (1999). Hybridization as a metric for the reaction coordinate of the chemical reaction. Concert in chemical reactions, Pure and Applied Chemistry. 289.

[19] Wang, N. Li, G.D. and Tang, Z.K., (2001). "Mono-sized and single-walled 4 Å carbon nanotubes", Chemical Physics Letters, 339: 47-52.

[20] Eres, G. Puretzky, A. Geohegan, D. and Cui, H., (2004). "In situ control of the catalyst efficiency in chemical vapor deposition of vertically aligned carbon nanotubes on predeposited metal catalyst films", Applied physics letters, 84: 1759-1761.

[21] Iijima, S. and Ichihashi, T., (1993). "Single-shell carbon nanotubes of 1-nm diameter", Nature, 363: 603-605.

[22] Yakobson, B., (1998). "Mechanical relaxation and “intramolecular plasticity” in carbon nanotubes", Applied physics letters, 72: 918-920.

[23] Falvo, M.R. Clary, G. Taylor, R. Chi, V. Brooks, F.P. Washburn, S. and Superfine, R., (1997). "Bending and buckling of carbon nanotubes under large strain", nature, 389: 582-584.

[24] Treacy, M.J. Ebbesen, T. and Gibson, J., (1996). "Exceptionally high Young's modulus observed for individual carbon nanotubes", Nature, 381: 678.

[25] Zhu, Y. Sekine, T. Kobayashi, T. Takazawa, E. Terrones, M. and Terrones, H., (1998). "Collapsing carbon nanotubes and diamond formation under shock waves", Chemical Physics Letters, 287: 689-693.

[26] Li, F. Cheng, H. Bai, S. Su, G. and Dresselhaus, M., (2000). "Tensile strength of single-walled carbon nanotubes directly measured from their macroscopic ropes", Applied physics letters, 77: 3161-3163.

[27] Wang, Z. Gao, R. Poncharal, P. De Heer, W. Dai, Z. and Pan, Z., (2001). "Mechanical and electrostatic properties of carbon nanotubes and nanowires", Materials Science and Engineering: C, 16: 3-10.

[28] Yu, M.-F. Files, B.S. Arepalli, S. and Ruoff, R.S., (2000). "Tensile loading of ropes of single wall carbon nanotubes and their mechanical properties", Physical review letters, 84: 5552.

[29] Baughman, R.H. Zakhidov, A.A. and De Heer, W.A., (2002). "Carbon nanotubes--the route toward applications", Science, 297: 787-792.

[30] Zhang, M. Atkinson, K.R. and Baughman, R.H., (2004). "Multifunctional carbon nanotube yarns by downsizing an ancient technology", Science, 306: 1358-1361.

[31] Inganäs, O. and Lundstrüm, I., (1999). "Carbon nanotube muscles", Science, 284: 1281-1282.

[32] Zhou, W. Winey, K.I. Fischer, J.E. Sreekumar, T. Kumar, S. and Kataura, H., (2004). "Out-of-plane mosaic of single-wall carbon nanotube films", Applied physics letters, 84: 2172-2174.

[33] Sreekumar, T. Liu, T. Kumar, S. Ericson, L.M. Hauge, R.H. and Smalley, R.E., (2003). "Single-wall carbon nanotube films", Chemistry of Materials, 15: 175-178.

[34] Kodama, H., (1981). "A scheme for three-dimensional display by automatic fabrication of three-dimensional model", J. IEICE, 64: 1981-1984.

[35] Bourell, D.L. Marcus, H.L. Barlow, J.W. Beaman, J.J. and Deckard, C.R., (1990). Multiple material systems for selective beam sintering, Google Patents.

[36] Burns, M., (1993). Automated fabrication: improving productivity in manufacturing: Prentice-Hall, Inc.

[37] Peiffer, R., (1993). "The laser stereolithography process—photosensitive materials and accuracy".

[38] Gibson, I. Rosen, D. and Stucker, B., (2014). Additive manufacturing technologies: 3D printing, rapid prototyping, and direct digital manufacturing: Springer.

[39] Liou, F.W., (2007). Rapid prototyping and engineering applications: a toolbox for prototype development: CRC Press.

[40] Berthelot, J.-M., (2012). Composite materials: mechanical behavior and structural analysis: Springer Science & Business Media.

[41] Chawla, K.K., (2012). Composite materials: science and engineering: Springer Science & Business Media.

[42] Kaw, A.K., (2005). Mechanics of composite materials: CRC press.

[43] Du, F. Scogna, R.C. Zhou, W. Brand, S. Fischer, J.E. and Winey, K.I., (2004). "Nanotube Networks in Polymer Nanocomposites: Rheology and Electrical Conductivity", Macromolecules, 37: 9048-9055.

[44] Bellayer, S. Gilman, J.W. Eidelman, N. Bourbigot, S. Flambard, X. Fox, D.M. De Long, H.C. and Trulove, P.C., (2005). "Preparation of homogeneously dispersed multiwalled carbon nanotube/polystyrene nanocomposites via melt extrusion using trialkyl imidazolium compatibilizer", Advanced Functional Materials, 15: 910-916.

[45] Chatterjee, T. Yurekli, K. Hadjiev, V.G. and Krishnamoorti, R., (2005). "Single-Walled Carbon Nanotube Dispersions in Poly (Ethylene Oxide)", Advanced Functional Materials, 15: 1832-1838.

[46] Co.Ltd., C.O.C., Technical data, China: Chinese Academy of Sciences.

[47] Zhang, J. Wang, Q. Wang, L. and Wang, A., (2007). "Manipulated dispersion of carbon nanotubes with derivatives of chitosan", Carbon, 45: 1917-1920.

[48] Moniruzzaman, M. and Winey, K.I., (2006). "Polymer Nanocomposites Containing Carbon Nanotubes", Macromolecules, 39: 5194-5205.

[49] O'connell, M.J., (2006). Carbon nanotubes: properties and applications: CRC press.

[50] Yu, Z. and Brus, L.E., (2000). "Reversible oxidation effect in Raman scattering from metallic single-wall carbon nanotubes", The Journal of Physical Chemistry A, 104: 10995-10999.

[51] Mawhinney, D.B. Naumenko, V. Kuznetsova, A. Yates, J.T. Liu, J. and Smalley, R., (2000). "Surface defect site density on single walled carbon nanotubes by titration", Chemical Physics Letters, 324: 213-216.

[52] Balasubramanian, K. and Burghard, M., (2005). "Chemically functionalized carbon nanotubes", Small, 1: 180-192.

[53] Teng, T.-P. Cheng, C.-M. and Pai, F.-Y., (2011). "Preparation and characterization of carbon nanofluid by a plasma arc nanoparticles synthesis system", Nanoscale research letters, 6: 293.

[54] Yazid, M.N.A.W.M. Sidik, N.A.C. Mamat, R. and Najafi, G., (2016). "A review of the impact of preparation on stability of carbon nanotube nanofluids", International Communications in Heat and Mass Transfer, 78: 253-263.

[55] Karousis, N. Tagmatarchis, N. and Tasis, D., (2010). "Current progress on the chemical modification of carbon nanotubes", Chemical Reviews, 110: 5366-5397.

[56] Nguyen, T. Petersen, E.J. Pellegrin, B. Gorham, J.M. Lam, T. Zhao, M. and Sung, L., (2017). "Impact of UV irradiation on multiwall carbon nanotubes in nanocomposites: Formation of entangled surface layer and mechanisms of release resistance", Carbon, 116: 191-200.

[57] Standard, A., (2003). "Standard test method for tensile properties of plastics", ASTM International. Designation: D, 638: 1-13.

[58] ASTM, G., (2015). 99-05," Standard Test Method for Wear Testing with a Pin-on-Disc Apparatus", ASTM International.

[59] Inc., F., (2016). Clear Photopolymer Resin for Form 1+ and Form 2 FLGPCL03 Material Properties, F. Inc.

[60] Yu, M.-F. Lourie, O. Dyer, M.J. Moloni, K. Kelly, T.F. and Ruoff, R.S., (2000). "Strength and breaking mechanism of multiwalled carbon nanotubes under tensile load", science, 287: 637-640.

[61] Torabi, A. Rahimi, A. and Ayatollahi, M., (2017). "Tensile fracture analysis of a ductile polymeric material weakened by U-notches", Polymer Testing.

[62] Askeland, D.R. and Phulé, P.P., (2006). The science and engineering of materials: Springer.

[63] Wan, H. Delale, F. and Shen, L., (2005). "Effect of CNT length and CNT-matrix interphase in carbon nanotube (CNT) reinforced composites", Mechanics Research Communications, 32: 481-489.

[64] Zhang, F. Shen, J. and Sun, J., (2004). "Processing and properties of carbon nanotubes-nano-WC-Co composites", Materials Science and Engineering: A, 381: 86-91.

[65] Nadiv, R. Shachar, G. Peretz-Damari, S. Varenik, M. Levy, I. Buzaglo, M. Ruse, E. and Regev, O., (2017). "Performance of nano-carbon loaded polymer composites: Dimensionality matters", Carbon.

[66] Perez, A.R.T. Roberson, D.A. and Wicker, R.B., (2014). "Fracture surface analysis of 3D-printed tensile specimens of novel ABS-based materials", Journal of Failure Analysis and Prevention, 14: 343-353.

[67] Chen, W. Li, F. Han, G. Xia, J. Wang, L. Tu, J. and Xu, Z., (2003). "Tribological behavior of carbon-nanotube-filled PTFE composites", Tribology Letters, 15: 275-278.

[68] Nam, T.H. Goto, K. Yamaguchi, Y. Premalal, E. Shimamura, Y. Inoue, Y. Naito, K. and Ogihara, S., (2015). "Effects of CNT diameter on mechanical properties of aligned CNT sheets and composites", Composites Part A: Applied Science and Manufacturing, 76: 289-298.

[69] Makowiec, M.E. and Blanchet, T.A., (2017). "Improved wear resistance of nanotube-and other carbon-filled PTFE composites", Wear, 374: 77-85.

APPENDIX-A

GRAPHS OF EXPERIMENTAL STUDIES

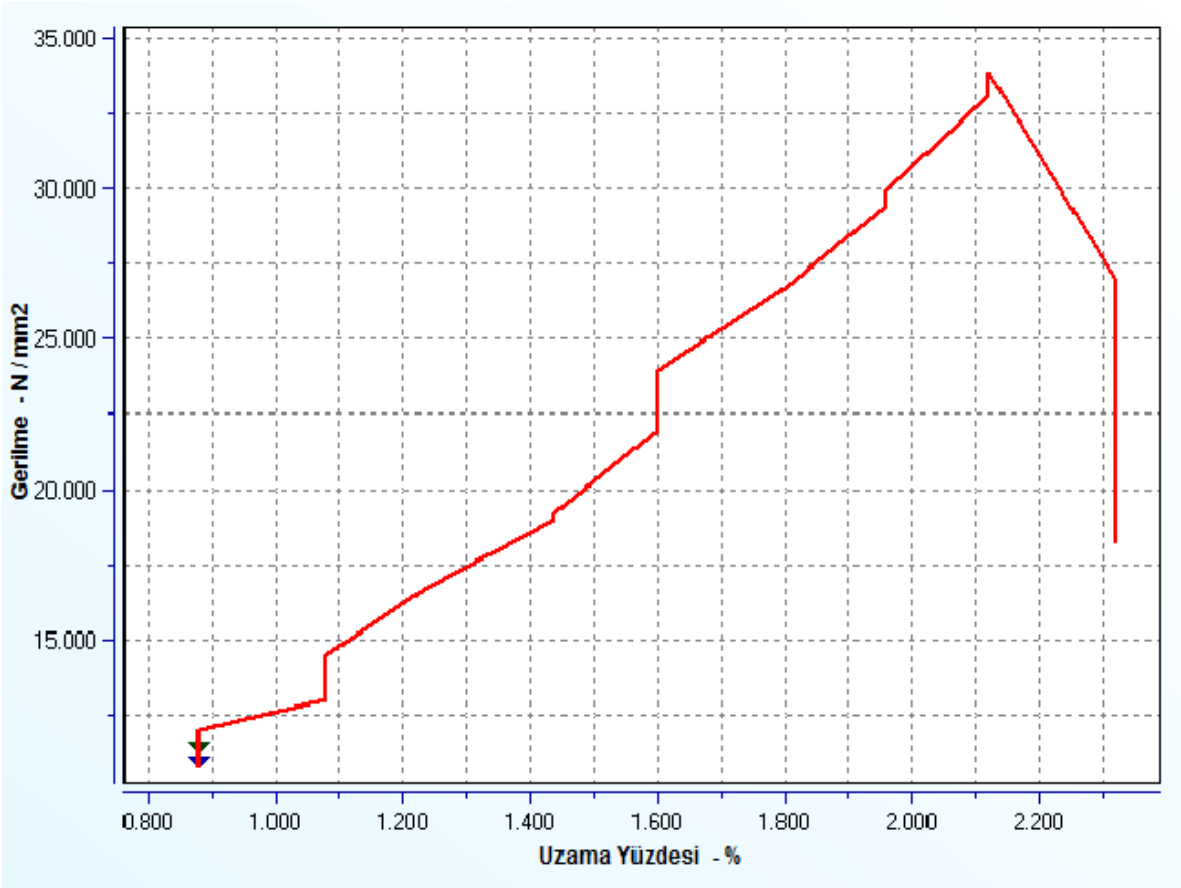

Tensile Test Graph of Base Specimen 1

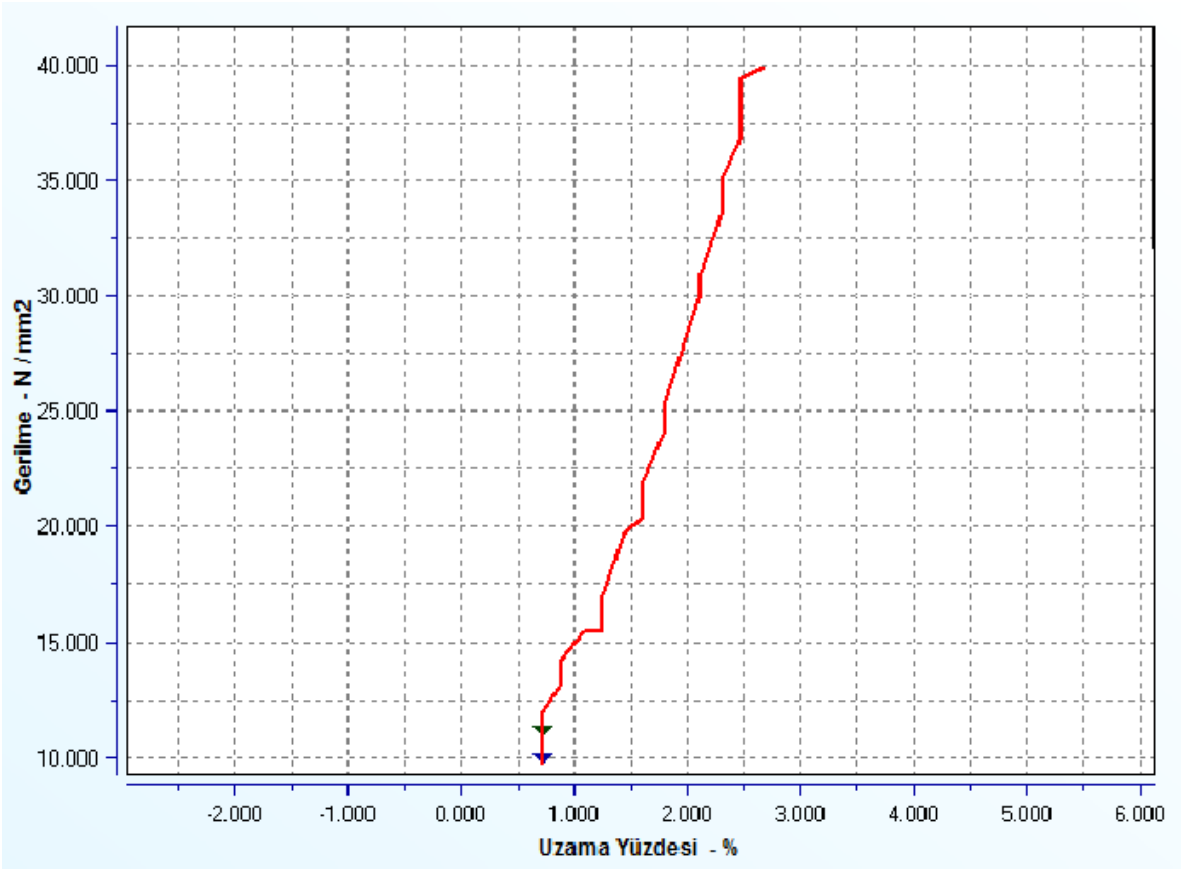

Tensile Test Graph of Base Specimen 2

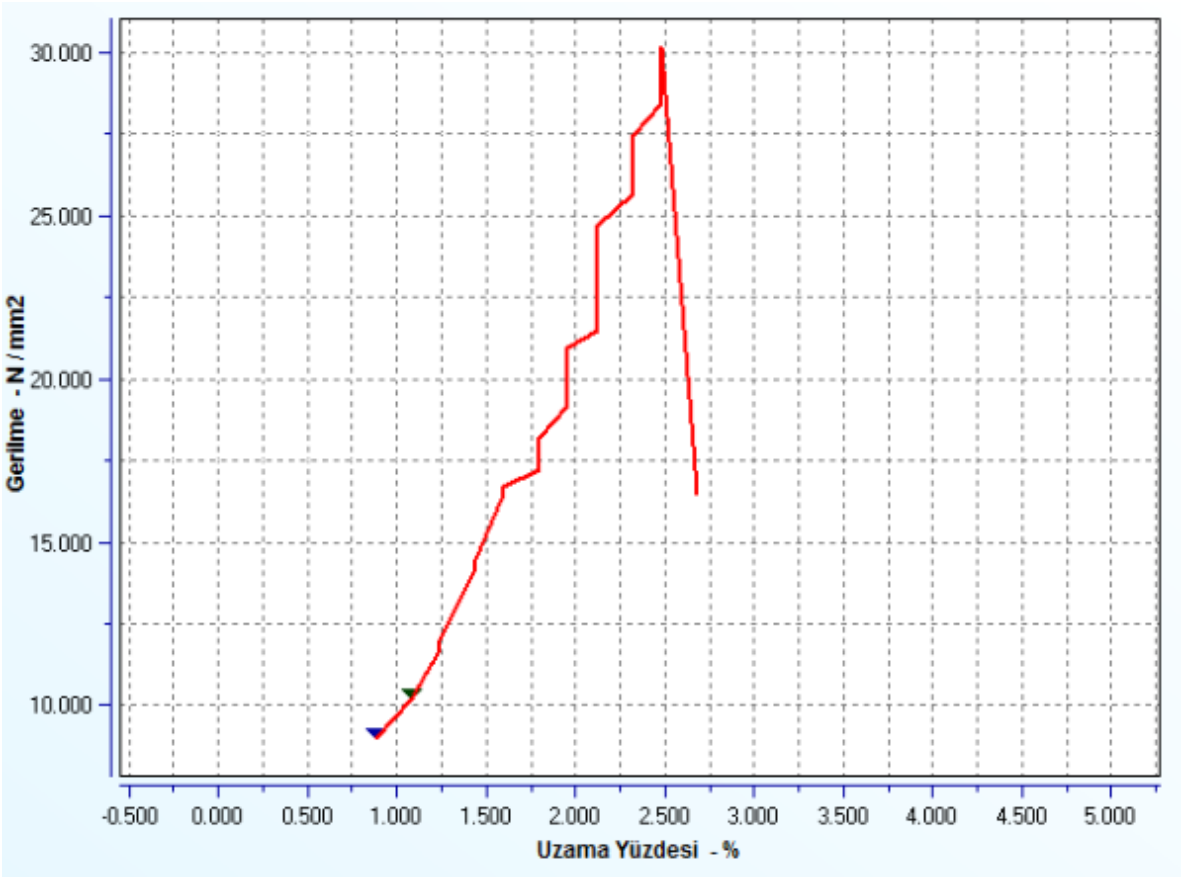

Tensile Test Graph of Base Specimen 3

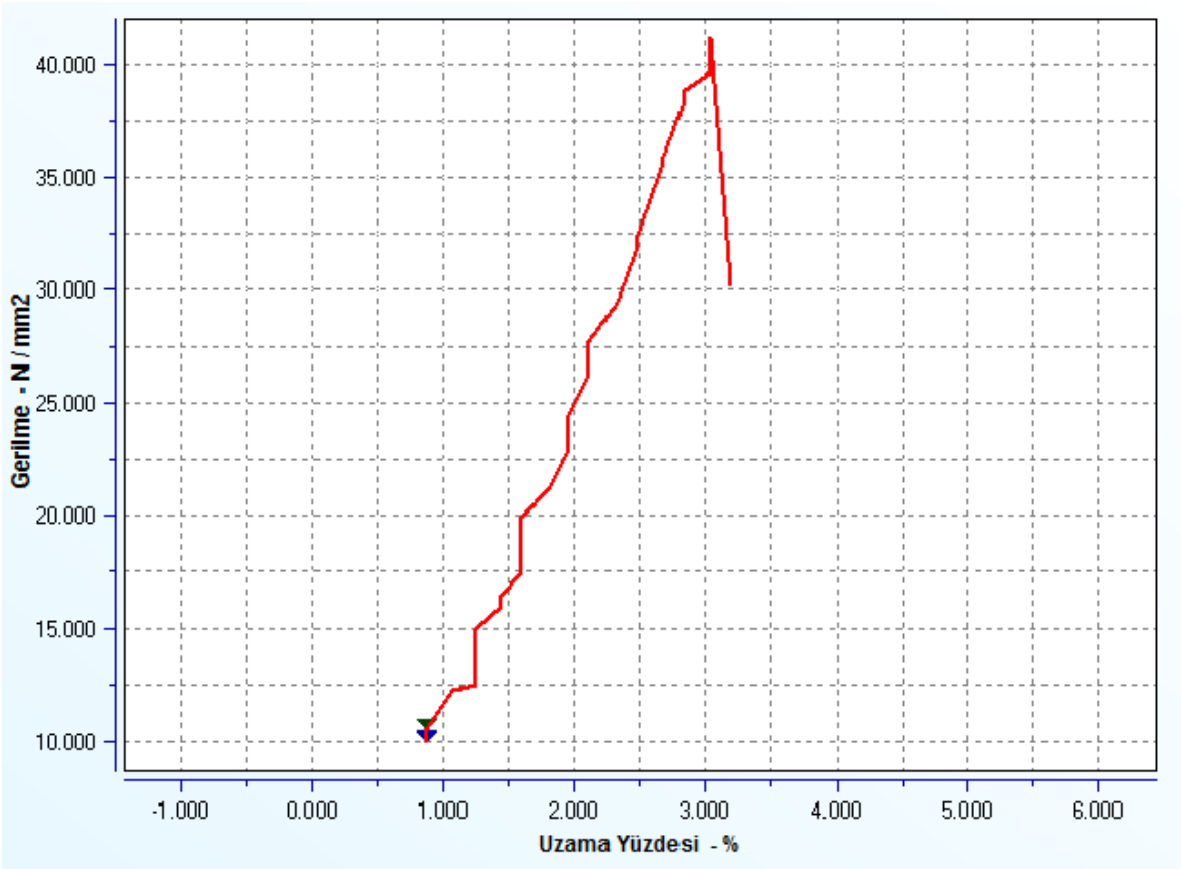

Tensile Test Graph of Base Specimen 4

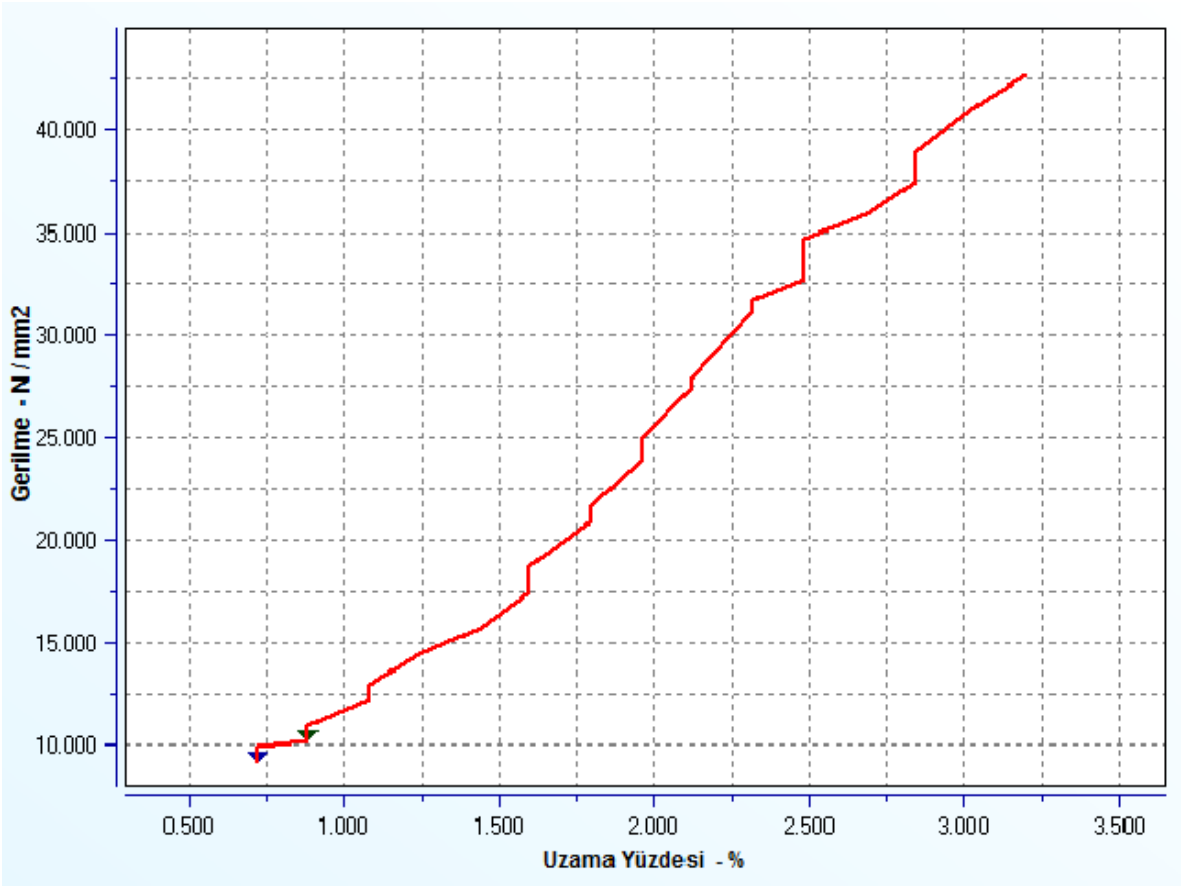

Tensile Test Graph of Base Specimen 5

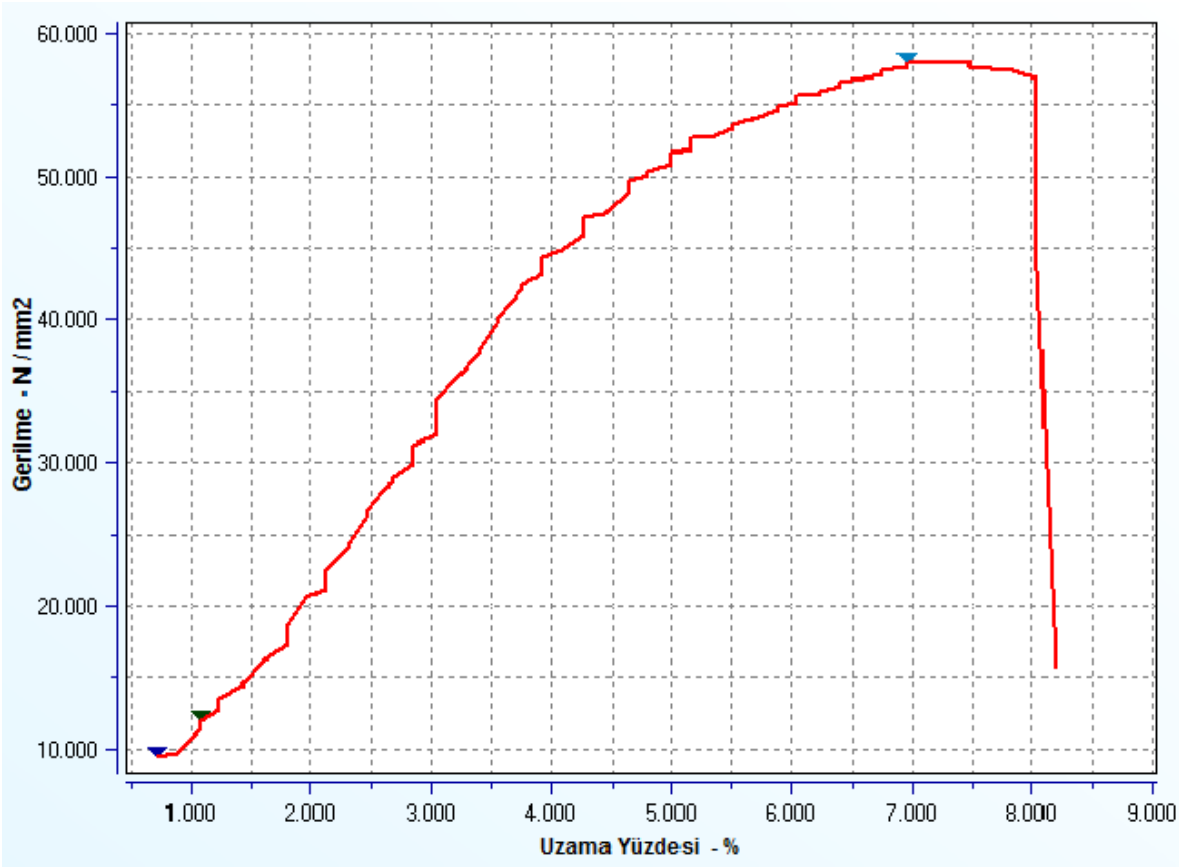

Tensile Test Graph of Reinforced Specimen 1

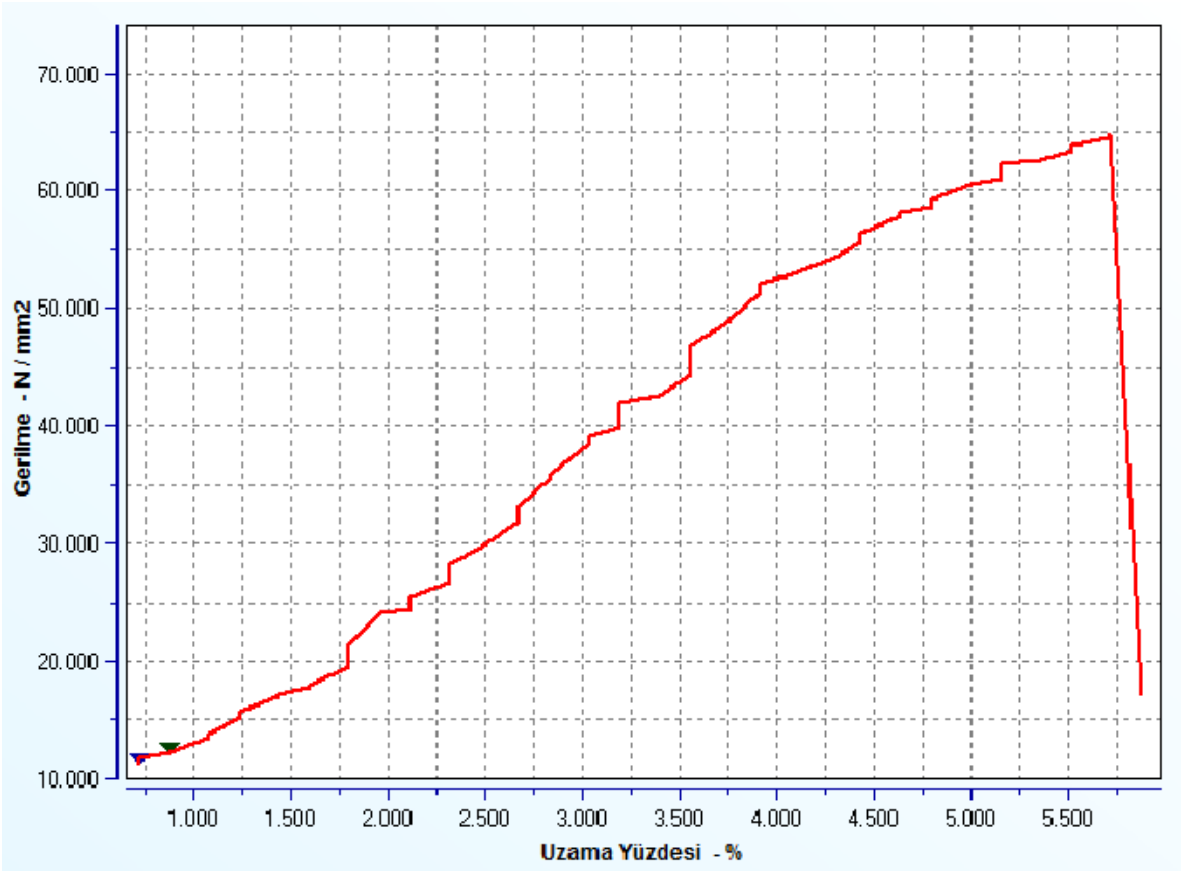

Tensile Test Graph of Reinforced Specimen 2

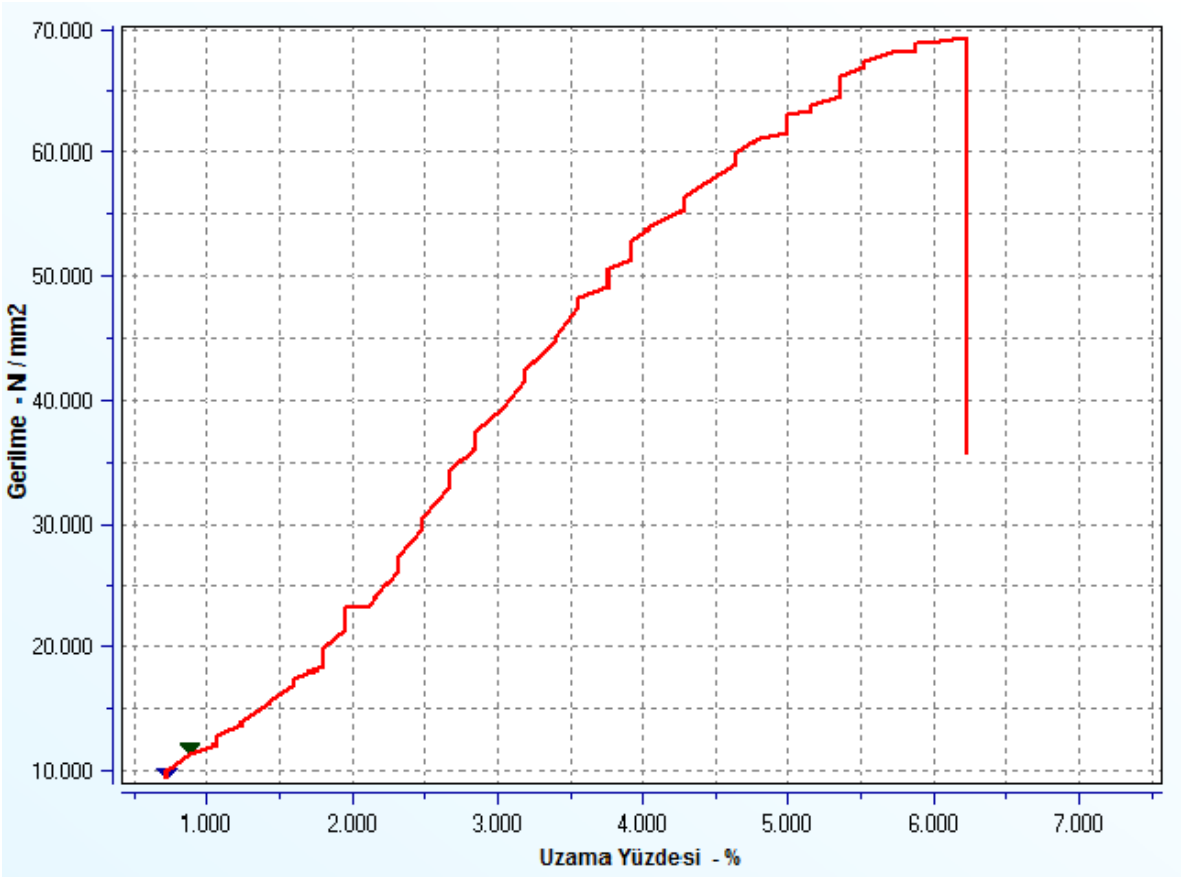

Tensile Test Graph of Reinforced Specimen 3

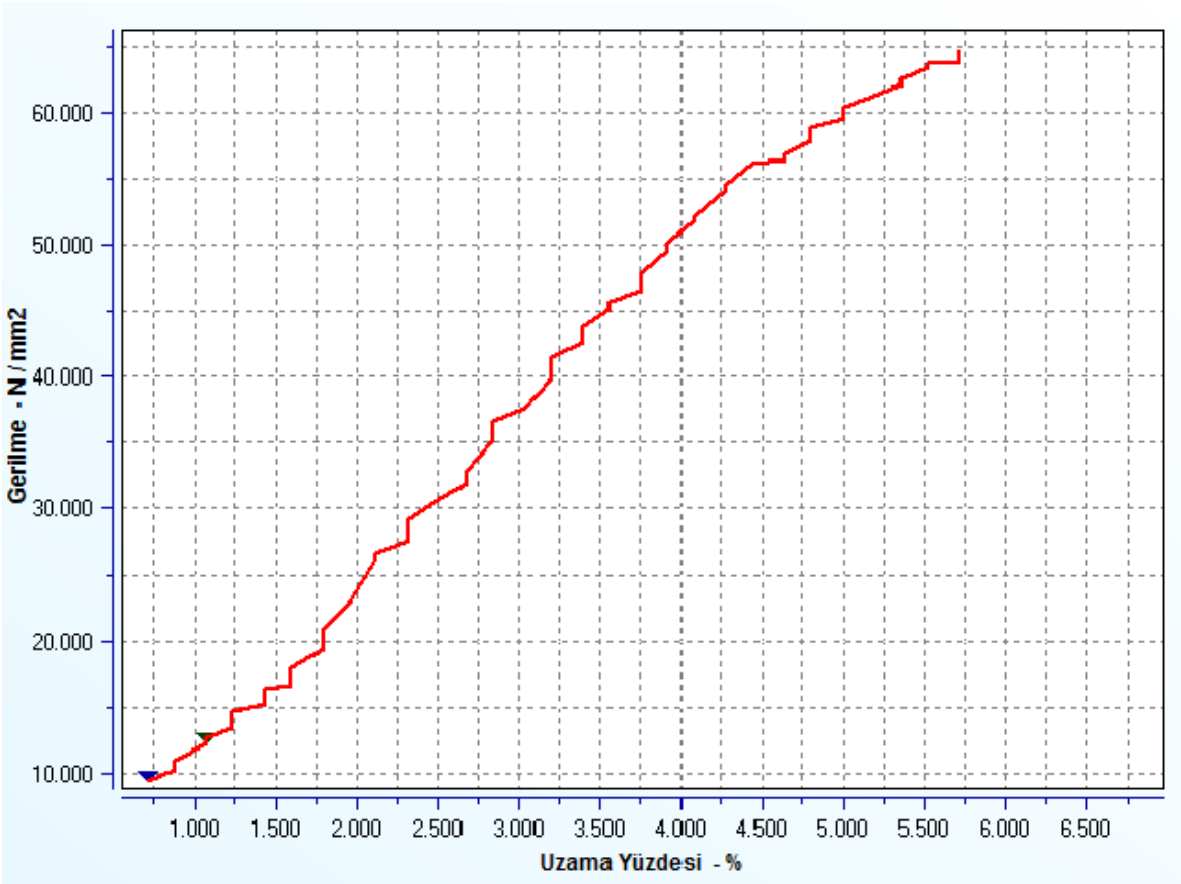

Tensile Test Graph of Reinforced Specimen 4

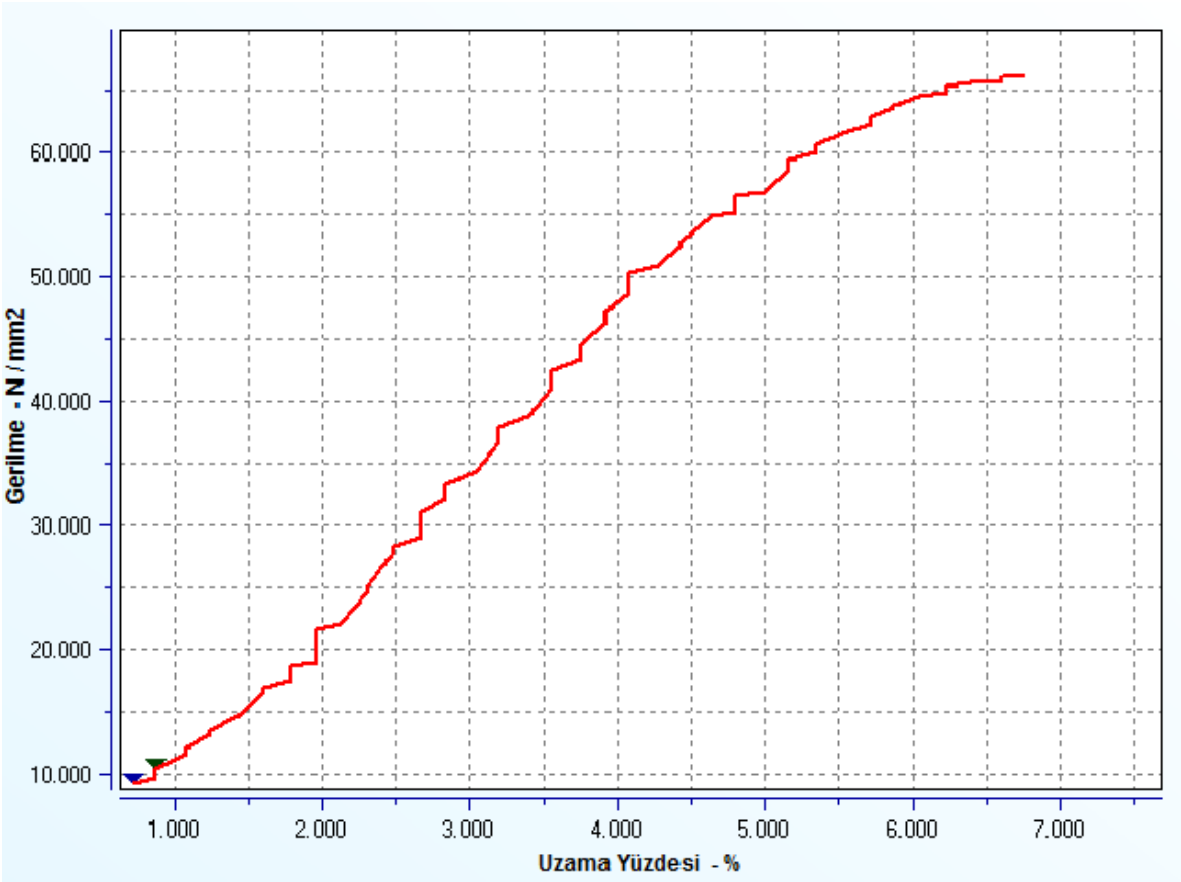

Tensile Test Graph of Reinforced Specimen 5

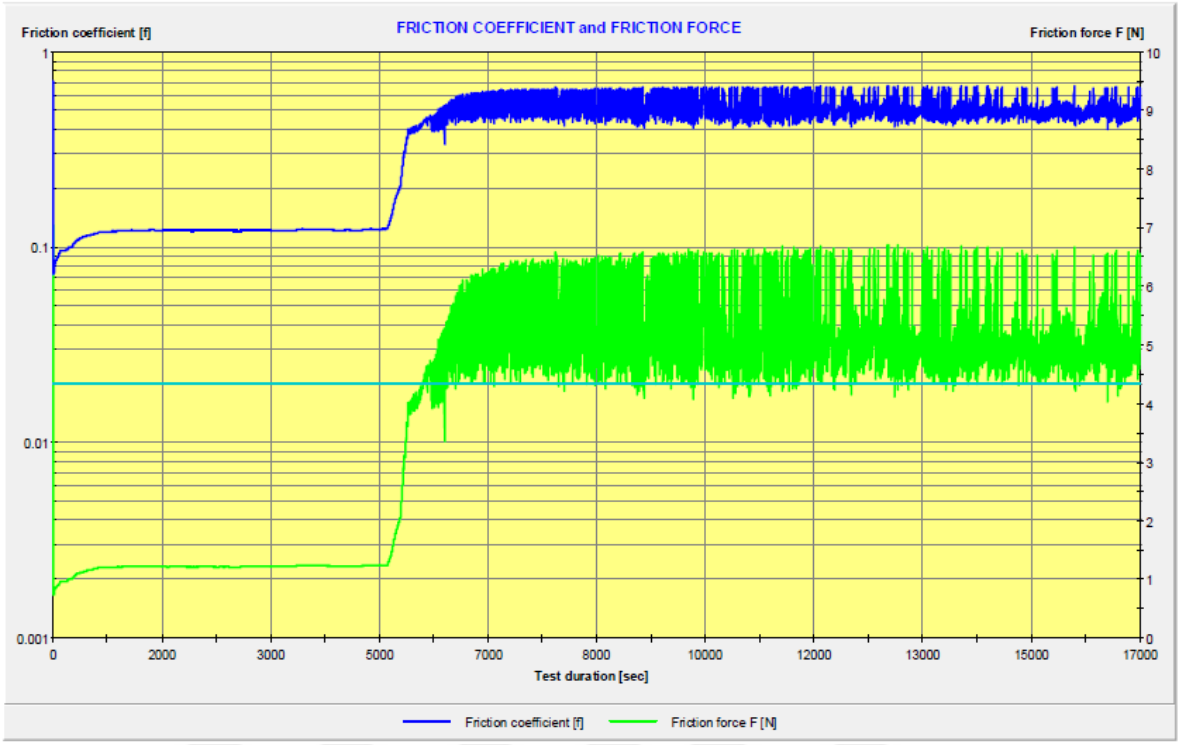

Wear Test Graph of Base Specimen for 2 mm radius

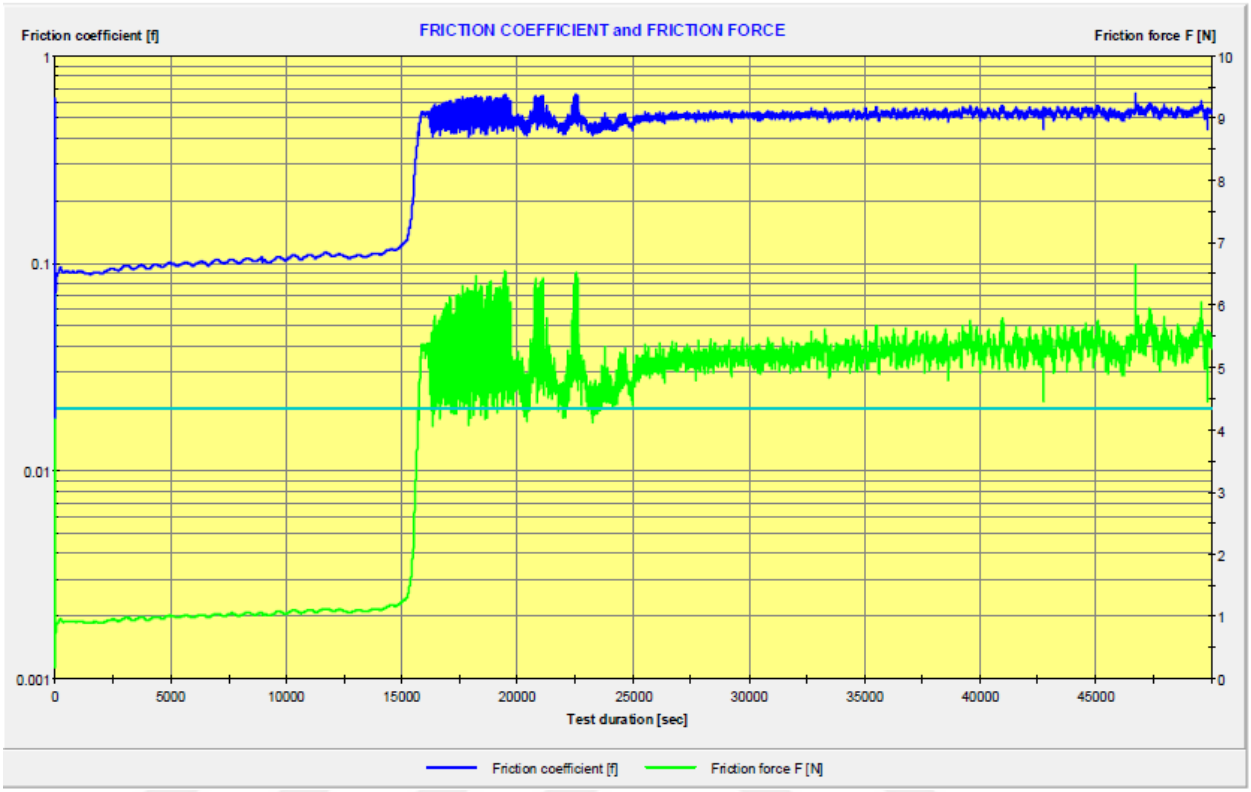

Wear Test Graph of Base Specimen for 4 mm radius

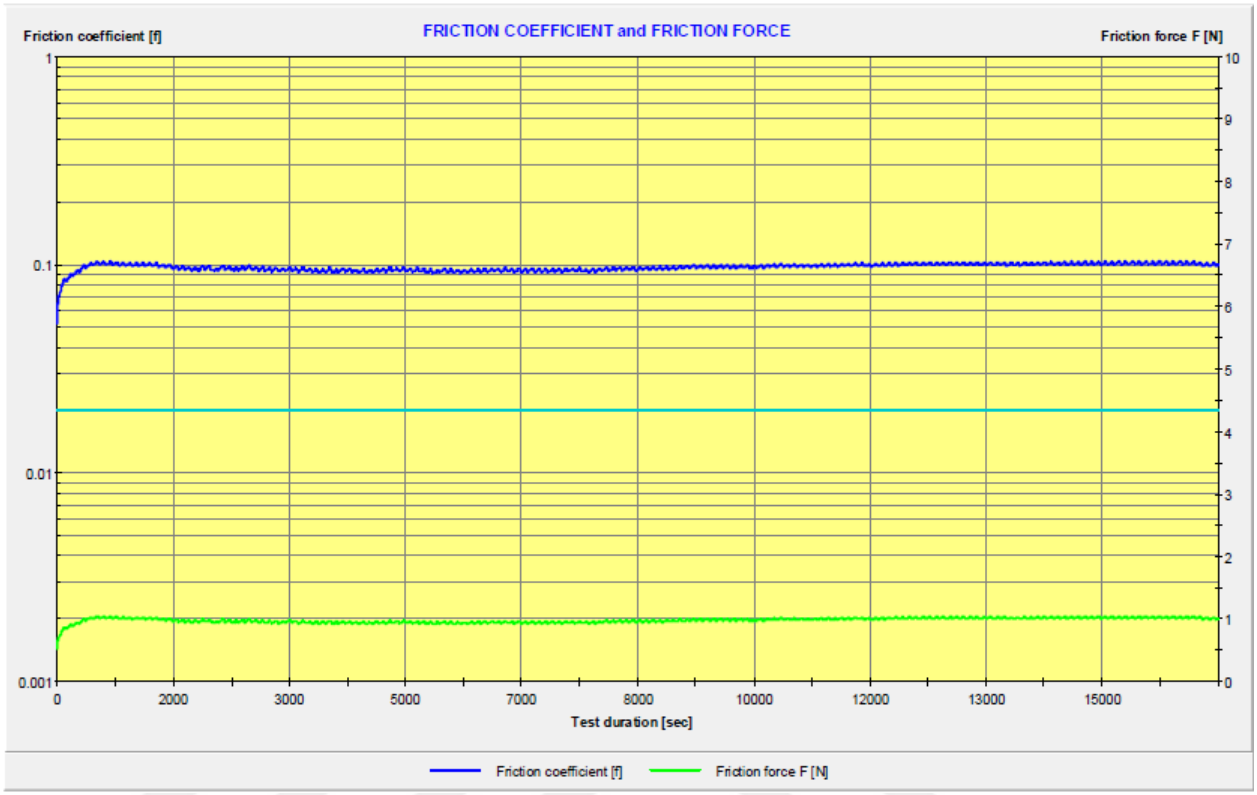

Wear Test Graph of Base Specimen for 6 mm radius

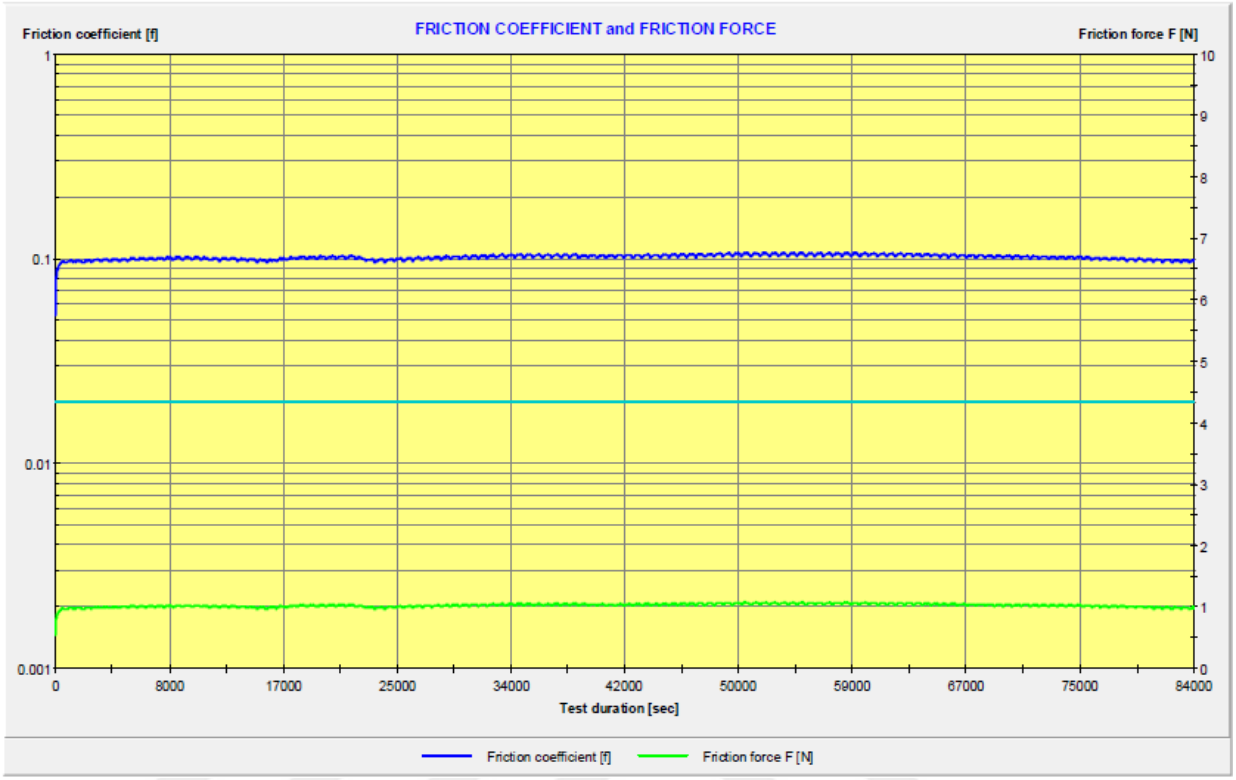

Wear Test Graph of Base Specimen for 8 mm radius

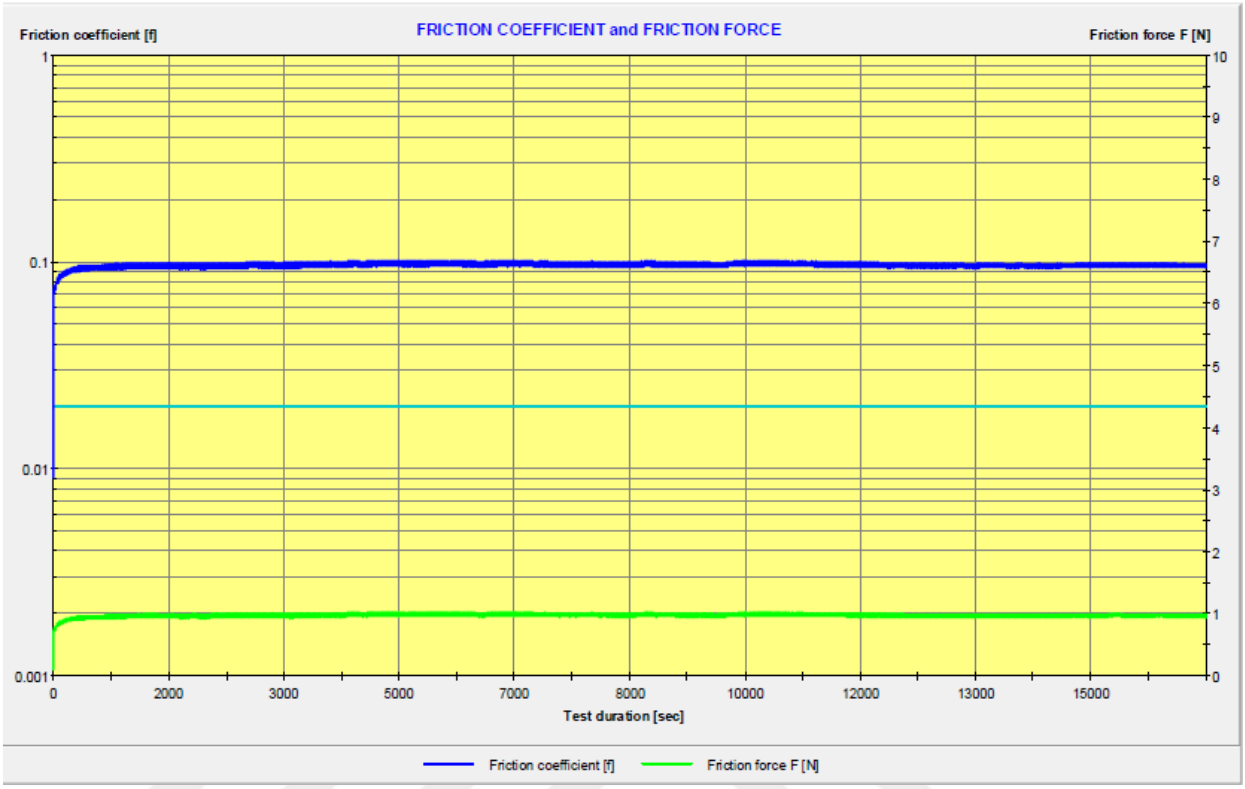

Wear Test Graph of Base Specimen for 10 mm radius

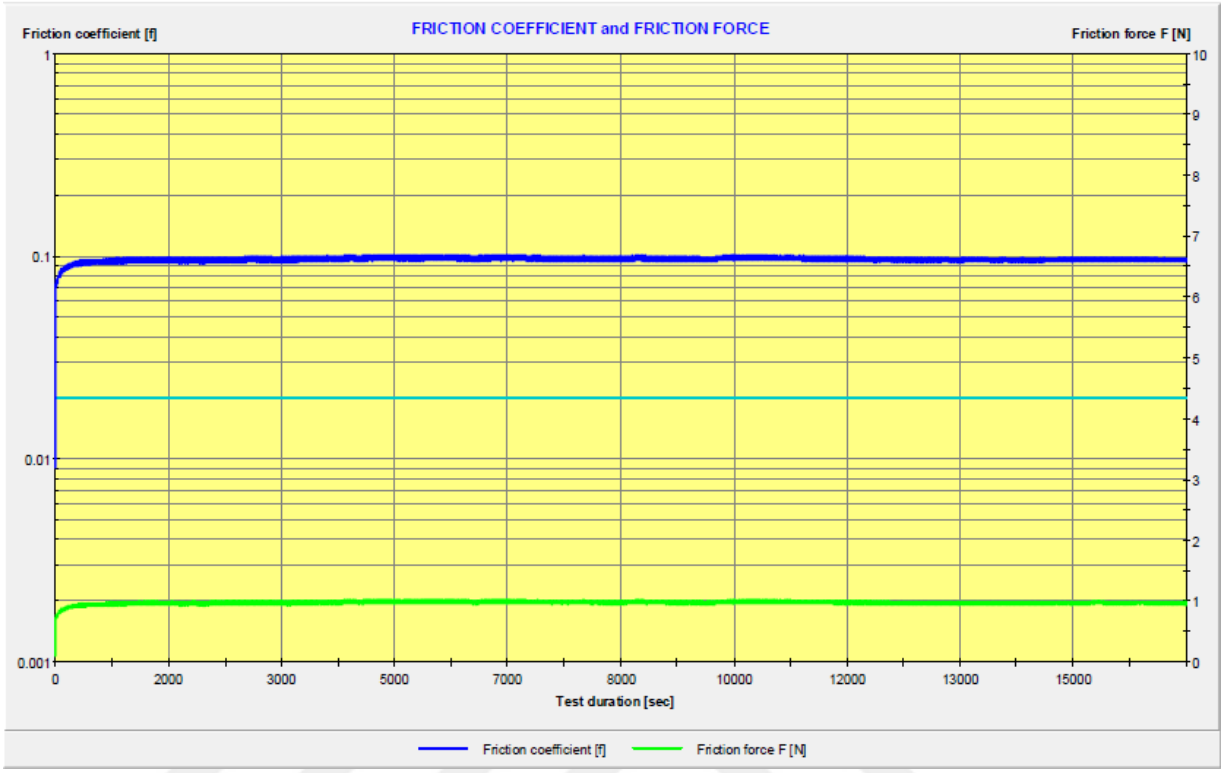

Wear Test Graph of Base Specimen for 12 mm radius

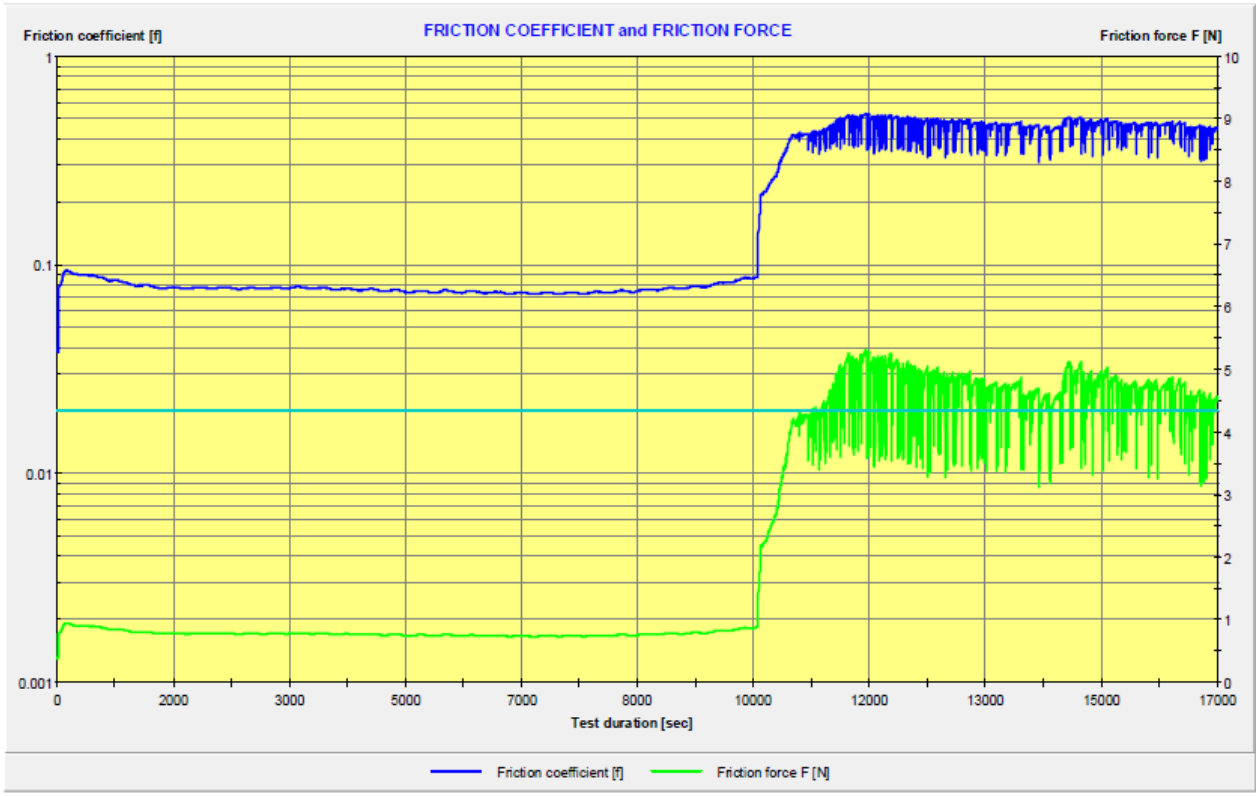

Wear Test Graph of Reinforced Specimen for 2 mm radius

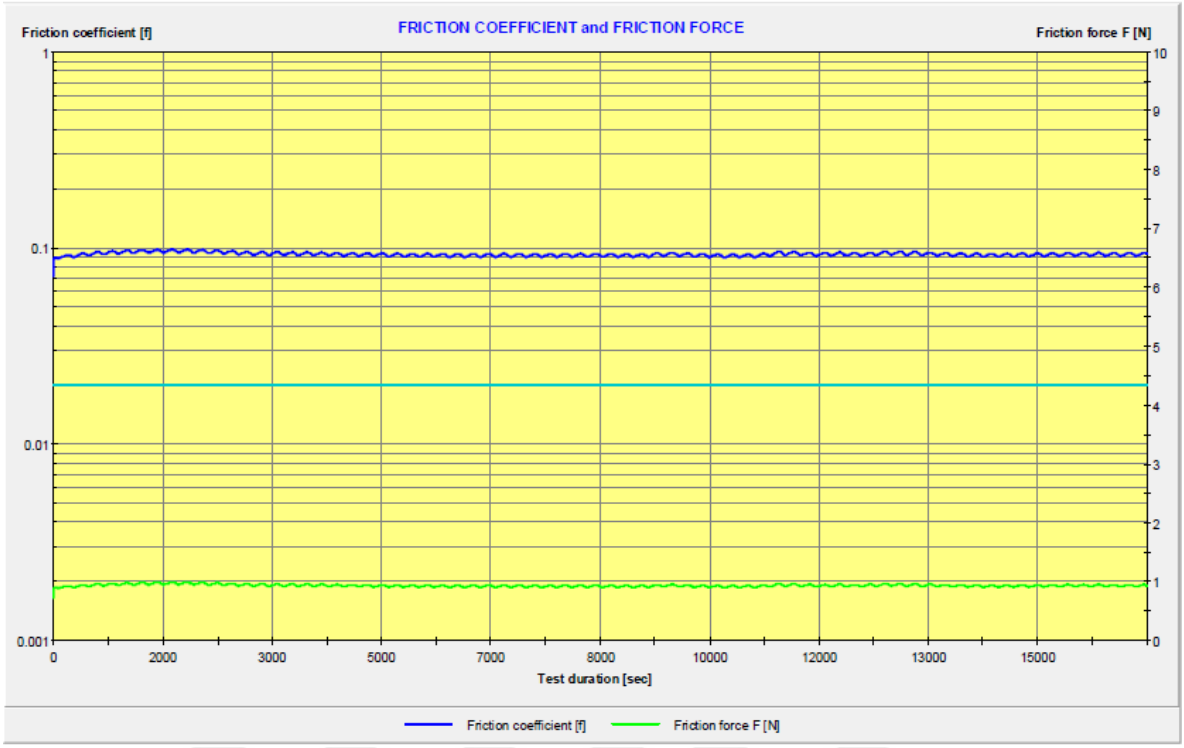

Wear Test Graph of Reinforced Specimen for 4 mm radius

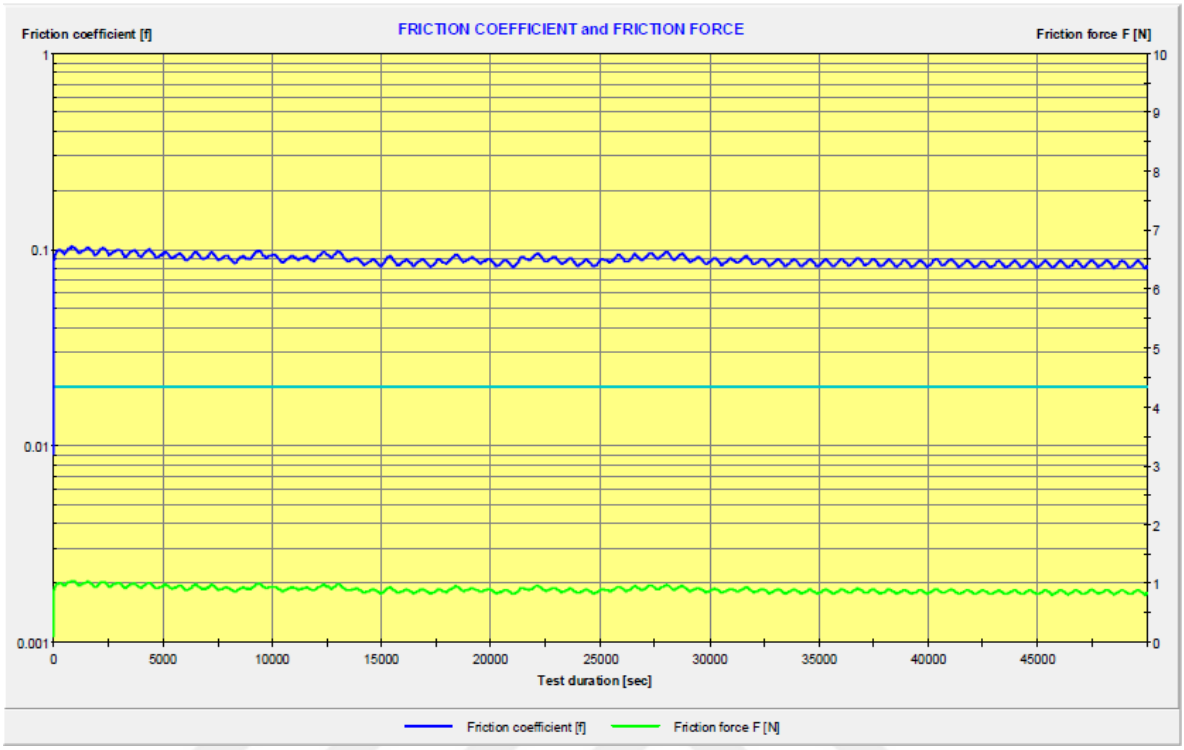

Wear Test Graph of Reinforced Specimen for 6 mm radius

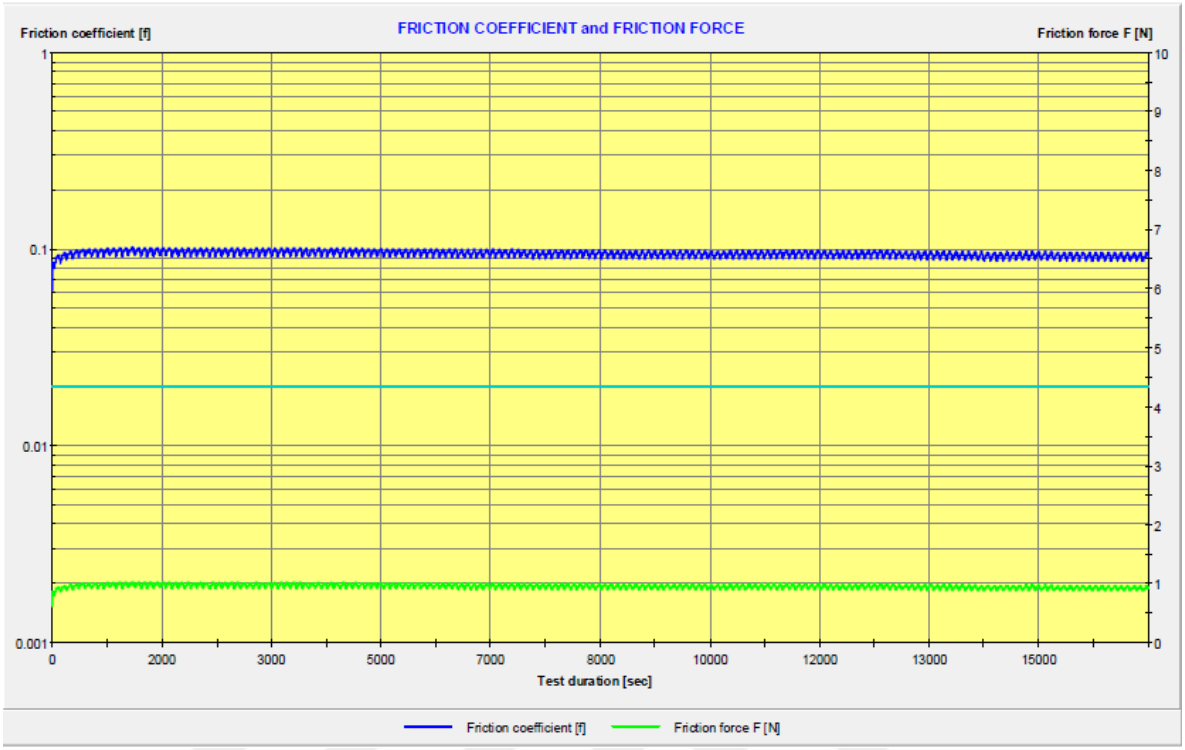

Wear Test Graph of Reinforced Specimen for 8 mm radius

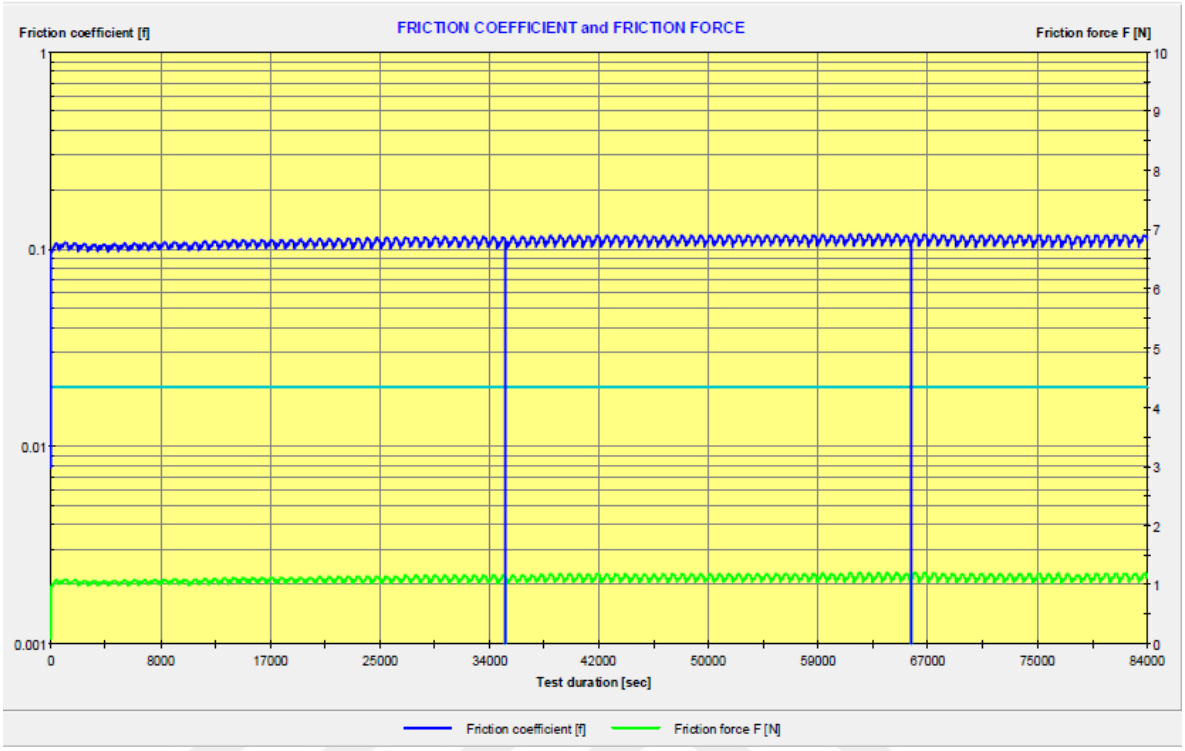

Wear Test Graph of Reinforced Specimen for 10 mm radius

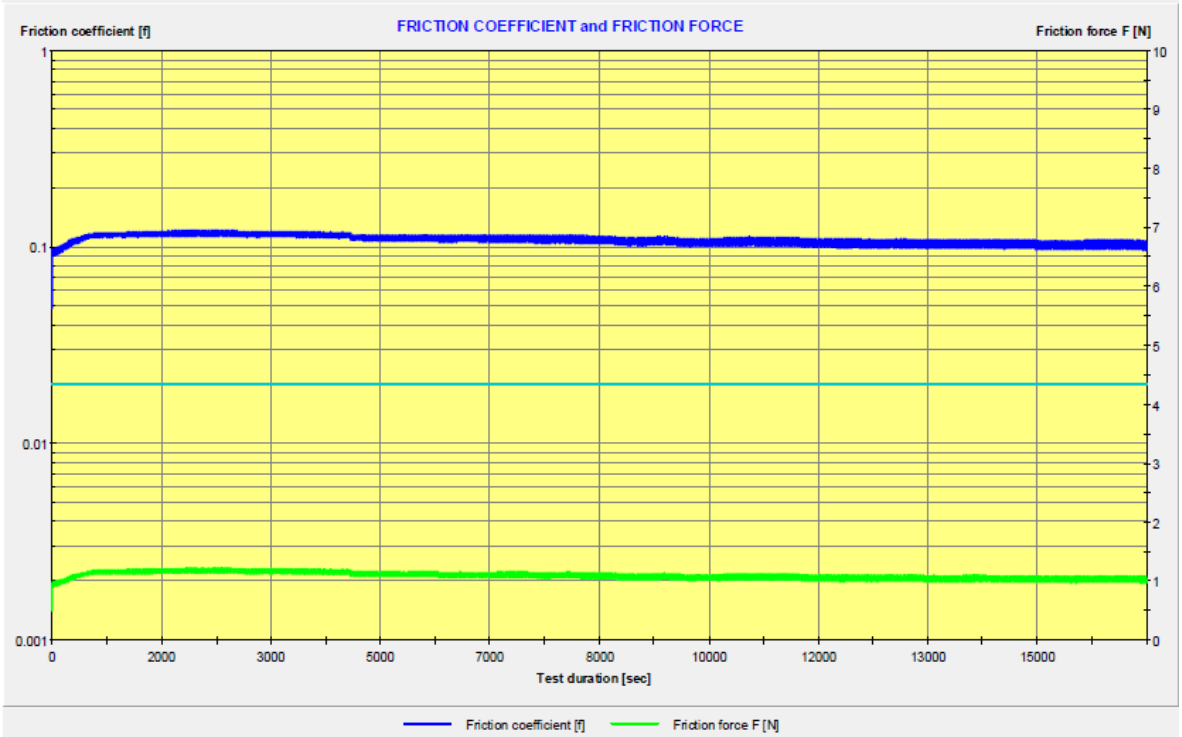

Wear Test Graph of Reinforced Specimen for 12 mm radius

CURRICULUM VITAE

PERSONAL INFORMATION

Name – Surname : Altuğ Akpınar
Date and Place of Birth : 12.02.1989 - ISTANBUL
Foreign Language : English
Email : altugakpinar13@gmail.com

EDUCATION

Degree	Area	School/University	Years
Master's Degree	Mechanical Engineering	Yıldız Technical University	2015-2017
Undergraduate	Mechanical Engineering	Kocaeli University	2010-2015
High School	Science	Ümraniye Anatolian High School	2003-2006